Molecular Vision 2025; 31:319-343 <http://www.molvis.org/molvis/v31/319>
Received 26 May 2025 | Accepted 1 October 2025 | Published 3 October 2025

Molecular insights into foveal hypoplasia: development, genetics, mechanisms, and models

Kevin Gregory-Evans, Cheryl Y. Gregory-Evans

Department of Ophthalmology and Visual Sciences, University of British Columbia, Vancouver Canada

The fovea is an anatomic specialization of the human retina critical for high visual acuity, color vision, and contrast sensitivity. The molecular and cellular pathways directing this focal topography are still to be determined. Abnormalities of the fovea (e.g., foveal hypoplasia in children) are considered a significant contributor to reduced quality of life. In addition, the fovea is often damaged in common retinal diseases, such as age-related macular degeneration and diabetic retinopathy, with a global economic burden of $500 billion USD. Currently, there are no treatments for foveal defects. Most genes contributing to foveal abnormalities have been identified but are yet to be characterized and studied. This is because common laboratory animals do not have a fovea, and only rare human tissue samples are available during the major phase of foveal maturation, from birth to the end of the fourth year of life. We discuss validation of the anole lizard, which has a foveal structure, for research studies into foveal development. Since foveal development continues after birth, it may be possible to stimulate new foveal maturation where there is developmental damage. From this review, we propose an evidence-based cellular mechanism that offers new possibilities for testing future therapies for foveal defects.

Foveal hypoplasia (FH) is a condition characterized by poor visual acuity, absence/partial absence of the foveal pit, reduced macular pigmentation, sometimes nystagmus, and absence of the foveal avascular zone (FAZ) [1]. FH in isolation is a rare genetic disorder [2-4]. It is, however, commonly found in other diseases, such as albinism, retinopathy of prematurity, aniridia syndrome, achromatopsia, incontinentia pigmenti, infantile nystagmus, familial exudative vitreoretinopathy (FEVR), and Best's disease [5-13]. Although there is no widely accepted statistic for incidence or prevalence, a recent study of over 900 patients revealed that FH was observed in 67.5% of cases of albinism, 21.8% cases with variants in the *PAX6* gene (aniridia syndrome), 6.8% of cases with variants in *SLC38A8* (foveal hypoplasia type 2), 3.5% of *FRMD7* (infantile nystagmus) variant cases, and 67.4% of achromatopsia cases with an atypical form of FH [14]. Other studies confirm that FH is more common in aniridia syndrome, including patients with chromosomal deletions, with a range from 41% to 90% [8,15,16]. The molecular and cellular mechanisms that drive the normal formation and maturation of the foveal specialization of the retina remain to be determined. Thus, the underlying pathophysiological processes that lead to foveal hypoplasia remain poorly understood. Since the fovea is often damaged in common retinal diseases, such as age-related macular degeneration [17] and diabetic retinopathy [18], with a global economic burden of over $500 billion USD [19,20], there is an urgent need to foster more research into understanding foveal development and loss of function in disease. Here, we review examples of how knowledge from foveal development has impacted the treatment of diseases such as age-related macular degeneration (AMD) and diabetic retinopathy.

Correspondence to: Cheryl Gregory-Evans, Department of Ophthalmology and Visual Sciences, University of British Columbia, Vancouver Canada, 2550 Willow Street, Vancouver BC, V5Z 3N9; Phone: 1-778-968-4349: email: cheryl.gregoryevans@ubc.ca

METHODS

Study participants and clinical assessment: This study was approved by the clinical research ethics board of the University of British Columbia and adhered to the tenets of the Declaration of Helsinki. Patients with foveal hypoplasia were examined by retinal specialists at the Eye Care Centre in Vancouver, Canada. Informed consent was obtained from all participants included in the study. Fundus imaging, autofluorescence, and spectral-domain optical coherence tomography (OCT; Heidelberg Engineering, Heidelberg, Germany) were performed.

Functional testing in anole lizards: This study was approved by the Animal Care Committee at the University of British Columbia in accordance with the guidelines established by the Canadian Council on Animal Care. Adult female anoles were purchased from Charles Sullivan (Nashville, TN). Animals were maintained at an ambient temperature of 28 °C, with 70% humidity on a 14:10 light/dark cycle. A diet of live crickets (*Acheta domesticus*), which had been dusted with a 2:1 mix of calcium powder/vitamin supplement (Rep-Cal

Research Laboratories, Los Gatos, CA), was provided every 2 days.

For OCT imaging, the anoles were fasted for 24 h before induction of general anesthesia with 30 mg/kg alfaxalone plus 0.1 mg/kg dexmedetomidine by subcutaneous injection into the cervical region. Topical local anesthetic (amethocaine drops) and 2.5% phenylephrine and 0.5% tropicamide were used to dilate the pupil. A drop of coupling reagent (Viscotears lubricating gel, Alcon, Fort Worth TX) was placed on the eye, and images were acquired using an image-guided OCT2 system (Phoenix-Micron, Bend, OR). For inducing injury to the choroid, anoles were anesthetized and dilating drops added as described above. After adding lubricating drops (Alcon Laboratories, Fort Worth, TX), the laser burns were induced (532-nm laser set at 500 mW for 5-s bursts) using the image-guided laser system (Micron IV, Phoenix-Micron, Bend, OR). After laser photocoagulation, the eyes were rinsed in saline, and antibiotic ointment was added. For the bait-capture test, anoles were fasted for 1 to 5 days in groups of eight before being offered a cricket to capture and eat. The number of anoles that caught the bait was recorded. For western blotting the proteins were extracted, separated by SDS polyacrylamide gel electrophoresis, and then transferred to Immobilon-FL membrane (Millipore Sigma, Etobicoke, ON, Canada) by standard methods. Membranes were incubated with a 1:100 dilution of a polyclonal PEDF antibody (PA5-75359, ThermoFisher Scientific, Toronto. ON, Canada) and visualized with a goat anti-rabbit secondary antibody (IRDy800 cw) using a Li-COR Odyssey detector (Mandel Scientific, Guelph, ON, Canada). ImageJ software was used to analyze band intensities relative to loading control (GAPDH).

For Western blot densitometry and quantitation of the bait capture test an unpaired two-tailed Student's *t* test was used for comparisons between treated and untreated groups. P values less than 0.05 were considered significant. All statistics were performed in either the GraphPad Prism 5.0

RESULTS AND DISCUSSION

Foveal anatomy: The human fovea (derived from the Latin *fovea*, meaning "pit") is seen on OCT as an indentation in the macular region of the retina that measures approximately 1,500 µm in diameter [21] (Figure 1A). The inner nuclear layer (INL, containing amacrine and horizontal cells), ganglion cell layer (GCL), and blood vessels slope away, so only the photoreceptor layer (ONL) and a few Müller cell processes are directly exposed to incoming light [22]. The density of cone photoreceptors in the fovea is higher than anywhere else in the retina and accounts for 8% of the activity in the primary visual cortex, even though it only represents approximately 0.01% of the retinal area [23]. At the center of the fovea is a rod photoreceptor-free area known as the foveola (cone density 200,000/mm^2) [24]. Here, the ONL has widened due to increased cone packing, and there is outer segment (OS) lengthening, seen as a small upward bend in the ellipsoid zone hyperreflective band (Figure 1A). At the center of the foveola, there is a 100-µm diameter region that is S-cone photoreceptor free [25], which corresponds to the phenomenon of foveal tritanopia (inability to distinguish blue from yellow) [26].

Clinical evaluation of fovea health: Noninvasive OCT has revolutionized the visualization of retinal pathologies, including foveal hypoplasia [27-30]. Furthermore, the use of high-resolution spectral-domain OCT has led to the development of the Leicester grading system by Irene Gottlob and colleagues, which is now used in routine practice to characterize the different severities of FH [31]. In the grading system, a normal foveal structure is composed of four elements, including complete excavation of the inner retinal layers, a foveal pit, widening of the ONL at the fovea, and OS lengthening (Figure 1A). The only difference to these features seen in grade 1 FH is a shallow pit due to incomplete excavation of the inner retinal layers. In grade 2 FH, there is no pit formation, but the ONL widening and OS lengthening are still present, showing that pit formation is not a prerequisite for cone packing. In grade 3, the only feature observed is ONL widening (Figure 1B), and in grade 4, there are no features of foveal specialization (Figure 1C), also known as foveal plana [31]. An atypical form of foveal hypoplasia is characterized on OCT imaging by disruption of the ellipsoid zone hyperreflective band (representing the photoreceptor inner segment ellipsoid highly packed with mitochondria), with a foveal pit or retention of the inner retinal layers.

However, some examples do not fit this classification, and perhaps a more nuanced grading system would be instructive when also considering the underlying genotype, the timing of foveal development, and the point at which development was arrested. One report examining FH in genotyped albinism cases revealed that some grade 1 patients had normal foveal pit parameters (OCA1 and OCA2 genotypes), suggesting the need to split the classification into grade 1a (normal pit) and grade 1b (partial pit) [32]. This has been recently added to the Leicester grading classification, although it has yet to be adopted more broadly [14]. Another report examined FH in *PAX6*-genotyped aniridia syndrome cases [8]. A patient was reported with a partial pit and ONL widening, but there was no OS lengthening (Figure 1D); thus, the presence of a pit and OS lengthening is not mutually coincident. Considering

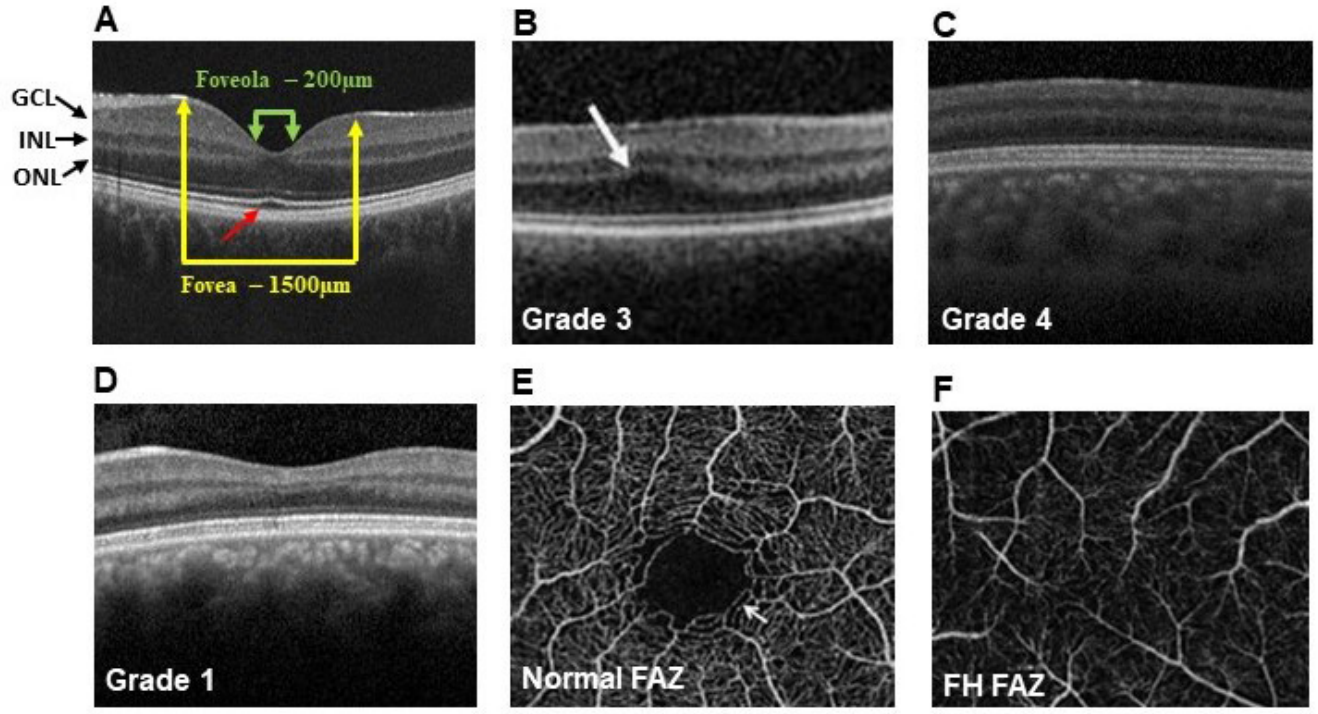

Figure 1. Optical coherence tomography (OCT) imaging in foveal hypoplasia (FH) cases. **A**: An OCT scan through a normal retina at the fovea. GCL, ganglion cell layer; INL, inner nuclear layer; ONL, outer nuclear layer. The yellow arrows define the size of the fovea. The green arrows show the size of the foveola in the center of the fovea. The red arrow denotes the outer segment lengthening feature of the fovea, seen as an upward bend in the hyperreflective ellipsoid zone band. **B**: This image shows grade 3 FH. The white arrow denotes the outer segment widening feature of the fovea. **C**: This image shows grade 4 FH with a typical flat retina (fovea plana) with no features of a normal fovea. **D**: This image shows atypical grade 1 FH with a shallow foveal pit but no outer segment lengthening. This image is from the daughter of the person in image **C**. **E**: An OCT angiography (OCTA) scan at the level of the superficial plexus in a retina with a normal foveal avascular zone (FAZ) indicated by a white arrow. **F**: An OCTA scan in a patient with FH showing the absence of the FAZ.

the timing of foveal development, the pit starts to form at 24 to 26 weeks' gestation, whereas OS lengthening does not start until after birth, reaching maturity in the fourth year of life. Therefore, it seems likely that other factors contribute to the specification of the four anatomic foveal elements, not directly related to genotype or the presence of a foveal pit.

Studies in families have revealed that the grade of FH in a parent does not necessarily reflect the outcome in offspring with the same genetic mutation [8]. For instance, the patient with grade 4 FH (shown in Figure 1C) had a child with grade 1 FH (Figure 1D). This is important because best-corrected visual acuities (BCVAs) in grade 1 and 2 FH tend to be better than those in grades 3 and 4, in particular correlating with OS length [14,33]. In the family described above, the BCVA logarithm of the minimum angle of resolution (logMAR) of the parent (aged 33 years) and child (aged 17 years) was 0.4/hand movements (HM) and 0.4/0.1, respectively. In another family, the parent (aged 52 years, BCVA 0.6/0.4) had grade 3 FH, and the child (aged 13 years, BCVA 1.3/1.3) had grade 4 FH, representing a worse outcome for the offspring [8]. Therefore, it is essential to visualize the health of the fovea as soon as possible to help predict likely visual outcomes. The introduction of handheld OCT devices [34,35] for use in preverbal children with nystagmus has been an important advance for monitoring and evaluating foveal maturation over time.

A key feature of FH is the absence of the FAZ, and this is not included in the OCT grading system. The addition of angiography to OCT (OCTA) allows a more detailed analysis of retinal vasculature stratified by layers, giving much improved visualization of the FAZ than is possible with traditional fluorescein angiography [36]. In normal retina, the FAZ can be clearly seen with OCTA at the level of the superficial plexus (Figure 1E), whereas in FH, the FAZ is absent with blood vessels crossing the retina (Figure 1F) [37]. OCT has also been used to evaluate foveal health in diabetic

retinopathy. Foveal neovascularization has been seen in 8% of cases with proliferative disease [38]. In addition, the size of the FAZ is increased before the onset of clinical signs of diabetic retinopathy [39,40]. Some studies in patients with age-related macular degeneration have also revealed a larger FAZ, foveal atrophy, and changes to the foveal microvascular circulation [41,42], alongside a reduction in the thickness of the inner retinal layers [43,44]. Finally, patients with retinopathy of prematurity have either a small or absent FAZ [45,46].

Foveal developmental timeline: Most knowledge relating to foveal development comes from extensive comparative morphological studies of human and primate eyes pioneered by Anita Hendrickson and colleagues [21,22,25,47-50]. In brief review, during ocular development, the presumptive fovea is first recognizable as a thickening of the GCL layer, beginning at around 11 to 12 weeks' gestation [51] and continues until 22 weeks' gestation, when it reaches five to seven cells deep (Figure 2A), with a single layer of cone photoreceptors in the ONL that lack inner and outer segments [21,52]. During this time, blood vessels have begun to grow along the horizontal meridian along the GCL/inner plexiform layer interface but do not extend into the location of the presumptive foveal pit. Stellate astrocytes and the ganglion cell plexus blood vessels form a perifoveal ring that is coincident with the rim of the incipient fovea [53]. This suggests that antiangiogenic factors repel blood vessel growth, allowing formation of the FAZ [53,54]. As development proceeds, the GCL and INL start to thin out by radial displacement and migration of cells, resulting in the start of foveal pit formation between 24 and 26 weeks' gestation (Figure 2B). By 28 to 29 weeks, the foveal pit is more prominent (GCL/INL each three to four cells thick), and the inner segments of photoreceptors have formed, along with the fibers of Henle (Figure 2C). At about 36 weeks, there is still a single layer of cone cells, but they now have short outer segments, and the GCL/INL has each reduced to two to three cells thick (Figure 2D). Shortly after birth, the foveal pit has further deepened, with the GCL/INL each reduced to one to two cells thick (Figure 2E). During the first postnatal year, cone photoreceptors migrate toward the foveal region, and the fibers of Henle are angled away from the central fovea. By 15 months of age, only a few cells in the GCL remain, allowing unimpeded access of incident light to the photoreceptors. The foveal cones have elongated and apical process from the retinal pigment epithelium (RPE) have intercalated between the outer segments. It is not until the fourth year of life that extensive cone-packing with elongation of the foveola cone outer segments is observed (Figure 2F). The ganglion cells in the foveal region receive input from single cone photoreceptors, which maximizes spatial resolution. In comparison, in the peripheral retina, a single ganglion cell receives input from multiple photoreceptors, maximizing sensitivity [55]. The postnatal foveal morphological developmental time frame corresponds with the age at which 20/20 visual acuity is achieved in children [56]. Based on comparative studies in monkeys, the human fovea is predicted to further mature, reaching its full potential by 5 to 8 years of age [24].

Foveal development and the FAZ: Work from Jan Provis and colleagues in primates has proposed that the presence of an FAZ is a critical element contributing to pit formation [22,53,57]. Human clinical imaging using OCT or OCTA (Figure 1E,F) provides the strongest evidence that without the FAZ, a foveal pit does not form and vice versa [28,37,58]. From 22 to 25 weeks, the developing blood vessels are excluded from the presumptive pit region where the FAZ will be established (Figure 2A,B), before the formation of the foveal depression [53,59]. One model proposes that pit formation requires the presence of an FAZ on which first intraocular pressure and then retinal stretch drive pit formation [60-63]. However, more recent molecular studies have revealed several antiangiogenic and axon guidance factors expressed by ganglion cells that inhibit astrocyte migration and blood vessel formation [53,64,65]. It is most likely that a combination of both molecular and mechanical stresses defines the avascular region of the retina and subsequent pit formation.

Molecular factors contributing to foveal development: In regions of high tissue specialization, such as the fovea, along with gene defects associated with the absence of a fovea, it is expected that during development, there will be differential patterns of gene expression (higher or lower levels of expression of specific genes driving foveal formation compared to nonfoveal tissue). Several tissue and single-cell studies have identified differentially expressed genes to gain further insight into the formation of the fovea and the contribution this may have to diseases affecting the foveo-macular region of the retina [64,66-76]. Most of these studies took tissue from adult donor eyes (human or primate), making the relevance of the data for identifying genes involved in the regulation of foveal development unclear. Comprehensive information was derived regarding candidate genes for adult-onset macular diseases and gene expression profiles in individual foveal cones. Across the data sets, there were commonalities in differentially expressed genes, adding rigor to the studies [71-73]. However, two studies analyzed gene expression changes at the time when the fovea was undergoing development [64,76], which have yielded some interesting candidate genes.

In the first study, macular versus nonmacular tissue was isolated from 19- to 20-week gestation eyes, the time when thickening of the ganglion cell layer marks the location of the incipient fovea. Complementary DNA generated from the tissue was then hybridized to human genome expression microarrays [64]. Differential gene expression was identified for 25 axon guidance genes and two antiangiogenic factors. The axon guidance genes included regulators of vascular

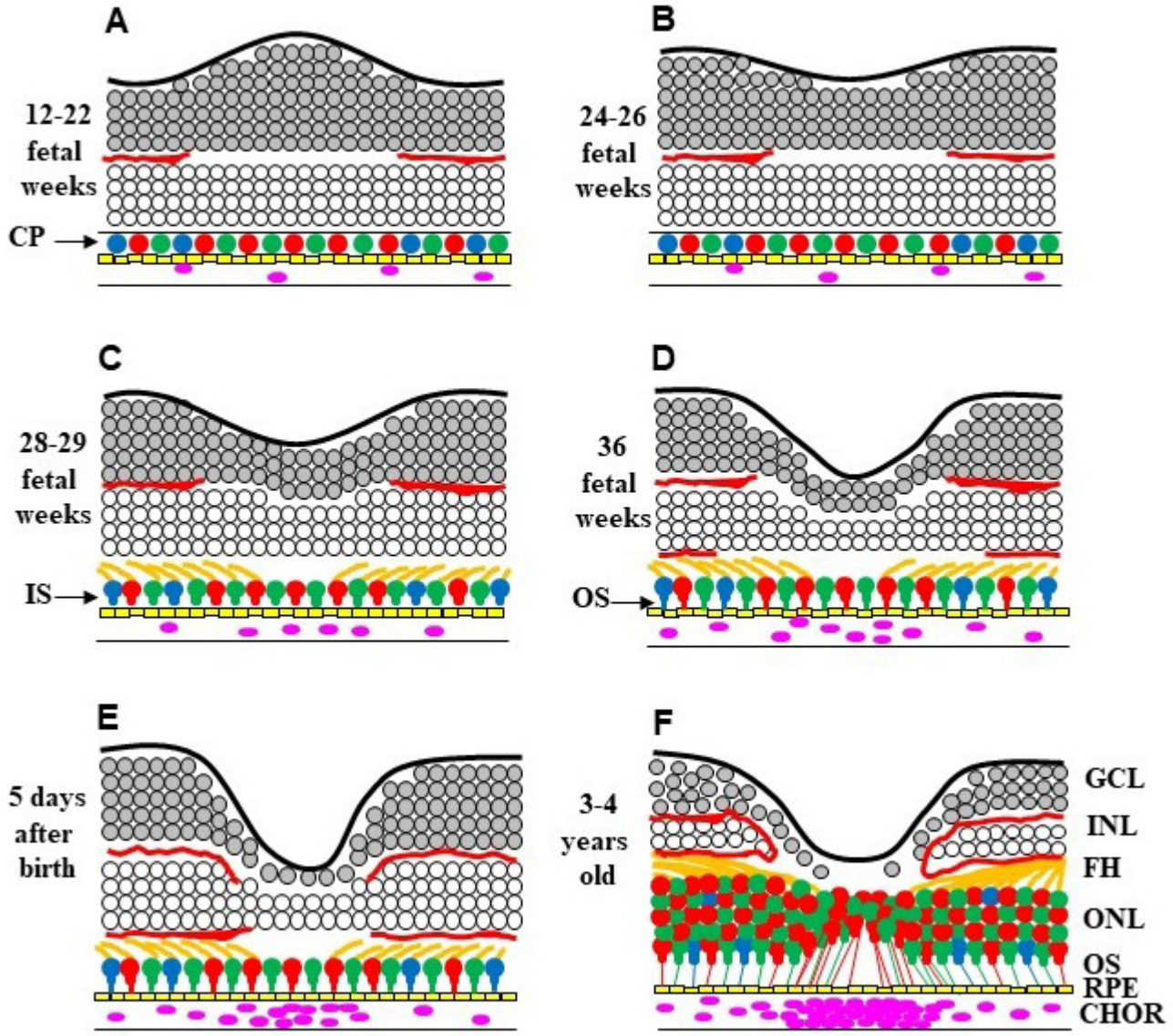

Figure 2. A representative schematic of the different stages of foveal development. **A**: This image shows ganglion cell layer (GCL) thickening at the position of the future foveal pit and ingrowth of blood vessels (red lines) between 12 and 22 weeks. Only a single row of cone photoreceptor (CP) cells is present. **B**: In this image the foveal depression starts to form between 24 and 26 weeks. **C**: In this image the GCL and inner nuclear layer (INL) start to thin out, and the fibers of Henle (FH) and the inner segments (ISs) of CP are formed. **D**: This image shows further excavation of the GCL and INL resulting in a deeper foveal pit, and the outer segments (OSs) of the CP are starting to form. **E**: This image shows the fovea shortly after birth, where the GCL and INL are one-to-two cells thick. Throughout development, the blood vessels do not encroach upon the foveal retina, forming the foveal avascular zone. **F**: This image shows the fovea by the fourth year of life, where the foveal region is packed with CPs in the outer nuclear layer (ONL) with elongated OSs. The choroid (CHOR) is filled with blood vessels to supply the outer retina and retinal pigment epithelium (RPE) with oxygen and nourishment. This is adapted from a previous publication by the authors [1].

development, such as ephrin, semaphorin, slit, and netrin gene families [77]. In a follow-up study, the authors found that differentially expressed ephrin-A6 repelled vessel growth in the FAZ region [65]. The two antiangiogenic factors that were upregulated in the macular samples were pigment epithelial-derived factor (PEDF) and natriuretic peptide precursor B. PEDF is a neurotrophic factor that decreases the survival of new endothelial cells in blood vessels through an apoptotic mechanism [78]. In addition, PEDF inhibits the activity of vascular endothelial growth factor (VEGF), a proangiogenic factor expressed in ganglion cells [79]. Localization of PEDF to the incipient foveal region [64] suggests it has an important role in preventing blood vessel formation in the developing FAZ. Natriuretic peptide precursor B is localized to ganglion cells, Müller glia, amacrine cells, and the RPE [80,81]. Its function is less well understood, but some natriuretic factors can inhibit VEGF-induced angiogenesis [82]. These studies suggest that expression of antiangiogenic factors and axon guidance factors plays a role in repelling blood vessel growth in the FAZ and could be the focus of future studies.

The second study used single-cell RNA sequencing and single-cell ATAC sequencing from the marmoset retina, and notable gene expression differences were observed between P0 neonatal foveal cones and peripheral cones compared to adult foveal and peripheral cones [76]. *RDH12*, *BACH1*, *AHR*, and *SOX6* were upregulated in neonatal foveal cones versus peripheral neonatal cones, but by adulthood, the differential expression was not maintained. Mutations in *RDH12* cause Leber congenital amaurosis, where an early feature is damage to the macula [83]. The BACH1 transcription factor represses Wnt signaling and angiogenesis [84], so it may be involved in the formation of the FAZ. Mutations in *AHR* have been found to cause isolated foveal hypoplasia with nystagmus [85], and *Ahr* is expressed in developing retinal ganglion cells in mice [86]. Thus, investigation of *AHR* expression in human or primate foveal development is warranted. *SOX4* was found to be upregulated in neonatal peripheral cones, whereas *SOX6* was elevated in foveal cones. While SOX4 is known to be involved in retinal ganglion cell differentiation and axon guidance [87], the role of SOX6 in the retina is unknown. Loss of *Sox6* in mice leads to dopaminergic neuronal degeneration [88], and reduced levels of SOX6 are seen in patients with Parkinson's disease [89]. Furthermore, Sox6 is expressed in differentiating and migrating cortical neurons in the developing brain but not the adult brain [90]. Thus, the role of SOX6 in neonatal foveal cones could be associated with the migration and packing of cones into the fovea. Further studies in model systems on *RDH12*, *BACH1*, *AHR*, and *SOX6* genes and their downstream targets could have a considerable impact on our understanding of foveal specification and their role in FH.

The candidate gene approach to target morphological observations in foveal development has also identified some interesting molecules. For example, the fibers of Henle (cone axons) undergo thinning and lengthening from mid-gestation to early childhood [21]. Similarly, cone photoreceptors undergo migration and outer segment lengthening. Thus, it could be hypothesized that growth factors may play a role in this process. It has been shown that fibroblast growth factor (FGF) 2 is expressed by cone photoreceptors during the postnatal period of outer segment elongation [91]. Additionally, a receptor for FGF signaling (FGF receptor 4) is also upregulated in cones postnatally and specifically in the fibers of Henle [92]. Growth factor studies in the FAZ have highlighted several candidates of interest. Transforming growth factor β has been shown to inhibit endothelial cell and Müller cell proliferation, which could be an important factor maintaining the developing avascular fovea [93]. In another study, VEGF messenger RNA was found to be expressed at high levels in astrocytes in advance of new blood vessel growth and in ganglion cells at the incipient fovea [94]. VEGF is usually upregulated in response to local developmental hypoxia [95]. There could be developmental hypoxia at the incipient foveal region due to increased neuronal maturation requirements of the developing foveal retina [96], yet VEGF does not induce blood vessel formation there. This could be for several reasons: (1) ganglion cells are supplied oxygen by diffusion from the choriocapillaris, so perhaps VEGF is having nonangiogenic effects on ganglion cells, such as neurotrophic/neuroprotective properties [97] or neuronal outgrowth of cell axons [98], and (2) antiangiogenic factors, such as PEDF, expressed at the FAZ overwhelm VEGF and thus inhibit astrocyte and endothelial cell proliferation [99]. Testing of these growth factors during foveal development will provide more concrete evidence of their roles in this process.

Genetic diseases exhibiting foveal hypoplasia: To date, 42 disease loci have been reported to include foveal hypoplasia as a phenotypic feature, and all but one of the genes have been identified (Table 1). More than half of the genes are associated with a syndromic form of albinism, including oculocutaneous albinism (8 genes), Hermansky-Pudlak syndrome (11 genes), and Chediak-Higashi syndrome (1 gene). Foveal hypoplasia is most frequently inherited in an autosomal recessive manner (31 diseases), whereas there are five cases of autosomal dominant transmission, five cases of X-linked inheritance, and one case of digenic inheritance.

Table 1. Human diseases associated with foveal hypoplasia.

Omim ID	Disease	Inheritance	Chromosome	Gene name
300500	Ocular albinism 1	XL	Xp22.3	*GRP143*
203100	Oculocutaneous albinism 1	AR	11q14.3	*TYR*
203200	Oculocutaneous albinism 2	AR	15q11.2-q12	*OCA2*
203290	Oculocutaneous albinism 3	AR	9p23	*TYRP1*
606574	Oculocutaneous albinism 4	AR	5p13.2	*SLC45A2*
615312	Oculocutaneous albinism 5	AR	4q24	unknown
113750	Oculocutaneous albinism 6	AR	15q21.1	*SLC24A5*
615179	Oculocutaneous albinism 7	AR	10q22.2-q22.3	*LRMDA*
619165	Oculocutaneous albinism 8	AR	13q32.1	*TYRP2/DCT*
203300	Hermansky-Pudlak 1	AR	10q23.1	*HPS1/BLOC3S1*
608233	Hermansky-Pudlak 2	AR	5q14.1	*AP3B1*
614072	Hermansky-Pudlak 3	AR	3q24	*HPS3/BLOC2S1*
614073	Hermansky-Pudlak 4	AR	22qcen-q12.3	*HSP4/BLOC3S2*
614074	Hermansky-Pudlak 5	AR	11p15-p13	*HPS5/BLOC2S2*
614075	Hermansky-Pudlak 6	AR	10q24.32	*HPS6/BLOC2S3*
614076	Hermansky-Pudlak 7	AR	6p22.3	*DTNBP1*
614077	Hermansky-Pudlak 8	AR	19q13	*BLOC1S3*
604310	Hermansky-Pudlak 9	AR	15q21.1	*PLDN/BLOC1S3*
617050	Hermansky-Pudlak 10	AR	19p13.3	*AP3D1*
619172	Hermansky-Pudlak 11	AR	6p24.3	*BLOC1S5*
214500	Chediak-Higashi	AR	1q42.1-q42.2	*LYST*
106210	Aniridia syndrome	AD	11p13	*PAX6*
609218	Foveal hypoplasia 2/FHONDA	AR	16q23.3-q24.1	*SLC38A8*
620958	Foveal hypoplasia 3	AR	7p21.1	*AHR*
216900	Achromatopsia 2	AR	2q11.2	*CNGA3*
262300	Achromatopsia 3	AR	8q21.3	*CNGB3*
613856	Achromatopsia 4	AR	1p13.3	*GNAT2*
613093	Achromatopsia 5	AR	10q23.33	*PDE6C*
610024	Achromatopsia 6	AR	12p12.3	*PDE6H*
616517	Achromatopsia 7	AR	1q23.3	*ATF6*
609049	Pierson syndrome	AR	3p21	*LAMB2*
607196	Amish microcephaly	AR	17q25.3	*SLC25A19*
310700	Congenital nystagmus	XL	Xq26.2	*FRMD7*
300600	Aland Eye Disease	XL	Xp11.23	*CACNA1F*
308300	Incontinentia pigmenti	XLD	Xq28	*IKBKG/NEMO*
133780	Familial exudative vitreo-Retinopathy (FEVR)	AD	11q14-q21	*FZD4*
152950		AD	10q23.33	*KIF11*
613310		AD	7q31.31	*TSPAN12*
601813		AD/AR	11q13.2	*LRP5*
305390		XL	Xp11.3	*NDP*
613703	Microphthalmia	digenic	12p13.1/8q22.1	*GDF3/GDF6*
153700	Best disease	AR	11q12.3	*BEST1*

Ocular albinism: Albinism occurs due to defects in the production of melanin or its metabolism [5]. Ocular albinism (OA), with a prevalence of 1:50,000, is phenotypically characterized by poor visual acuity due to foveal hypoplasia and is frequently associated with horizontal nystagmus, photophobia, and strabismus caused by optic chiasm misrouting [100]. OA is caused by a mutation in the *GPR143* gene, which encodes a G protein-coupled receptor in the melanosome membrane of RPE cells [101,102]. GPR143 binds tyrosinase and is involved in melanosome maturation [103]. Female carriers of *GPR143* variants often show a mild phenotype with reduced visual acuity. In one report, "mud-splatter" pigmentation of the fundus was observed due to random patches of X-inactivation in the RPE, iris transillumination defects, and retained inner retina layers at the fovea [104]. We have also seen phenotypic changes in a patient with confirmed OA disease (*GPR143* c.885+748G>A, a known pathogenic variant [105]). This patient had reduced visual acuity (20/25 in both eyes), streaky RPE pigmentation on fundus and autofluorescence imaging, and a thinner-than-normal central fovea (left, 182 µm; right, 185 µm; normal thickness, ≥210 µm) due to reduced widening of the ONL (Figure 3). This corresponds to grade 1b FH.

Oculocutaneous albinism: Eight oculocutaneous albinism (OCA) loci cause hypopigmentation in the eyes, hair, and skin with an estimated global prevalence of 1:12,000 to 15,000 [106], although this does vary depending on subtype and geographical location. OCA1 (1:40,000) is caused by mutations in the tyrosinase gene (*TYR*), which catalyzes several rate-limiting steps in the production of melanin [103]. OCA1 is subdivided into OCA1A (complete lack of tyrosinase activity) and OCA1B (reduced tyrosinase activity) [100]. OCA2 (1:40,000 worldwide and 1:1,500-3,900 in sub-Saharan Africa) has a highly variable phenotype and is caused by mutations in the *OCA2/P* gene that regulate melanosome pH [107,108]. OCA3 (1:8,500 in Africa, but rarer worldwide) is caused by mutations in the tyrosinase-related protein 1 (*TYRP1*) gene. TYRP1 is a catalase involved in maintaining the stability of the TYR protein and is involved in the formation of melanosome structure [109,110]. OCA4 (1:100,000), although rare, is the most common form of syndromic albinism (24% of cases) in Japan [111]. OCA4 is caused by mutations in the solute carrier family 45, member 2 (*SLC45A2*), resulting in retention of the protein in the endoplasmic reticulum [112]. SLC45A2 functions as a proton/glucose exporter that increases the luminal pH of melanosomes, which inhibits melanin biosynthesis [113]. OCA5 was described in a single Pakistani family that was mapped to chromosome 4q24, but the causative gene has not yet been identified [114]. OCA6 is rare and caused by mutations in the solute carrier family 24, member 5 (*SLC24A5*) [115]. SLC24A5, a potassium-dependent sodium/calcium exchanger located in the melanosome membrane [116], is involved in melanosome maturation and melanin synthesis [117]. OCA7 was described in a family from the Faroe Islands and mapped to chromosome 10q22.2-q22.3 [118]. The causative gene was identified as *C10orf11*, now renamed LRMDA (leucine-rich melanocyte differentiation-associated) protein, which is a melanocyte differentiation gene involved in melanosome biogenesis [119]. Subsequent mutations were identified in several Dutch, Kurdish, and Lithuanian patients [118,120]. OCA8 is another rare disease caused by mutations in the dopachrome tautomerase (*DCT*) gene [121,122], which is also known as the tyrosinase-related protein 2 (*TYRP2*) gene [123]. DCT/TYRP2 catalyzes the tautomerization of L-DOPAchrome (the red melanin precursor protein) into 5,6-dihydroxyindole-2-carboxylic acid, a colorless building block of eumelanin [124,125].

Hermansky-Pudlak syndrome: Hermansky-Pudlak syndrome (HPS) is a rare autosomal recessive disorder with a prevalence of approximately 1 to 9 per 1,000,000 (Orphanet). HPS is characterized by oculocutaneous albinism with bleeding diathesis (prolonged bleeding times and/or easy bruising) [126] and can be associated with pulmonary fibrosis [127], granulomatous colitis [128], or immunodeficiency [129]. The disease is genetically heterogeneous, with 11 known loci, and all the genes have been identified (Table 1). The protein products of these genes are involved in membrane trafficking required by lysosome-related organelles such as melanosomes in melanocytes and delta granules in platelets [130,131]. Based on genotype-phenotype correlations, the individual genes can be grouped into one of four multi-subunit complexes known as BLOC-1, BLOC-2, BLOC-3, and AP-3 [131]. This functional grouping aids in clinical management and enhances understanding of the pathobiology underlying lysosome-related organelle damage. BLOC-1 deficiency: there are eight subunits in this complex, of which four (DTNBP1, BLOC1S3, PLDN, and BLOC1S5) are known to be defective in HPS types 7, 8, 9, and 11, respectively [132]. BLOC-1 patients exhibit typical ocular albinism with bleeding diathesis and colitis. BLOC-2 deficiency: this complex consists of three subunit proteins (HPS3, HPS5, and HSP6) that cause HSP types 3, 5, and 6, respectively [133]. Patients with BLOC-2 deficiency experience the mildest symptoms, including decreased visual acuity with age, nystagmus, minimal skin hypopigmentation, and mild bleeding complications. BLOC-3 deficiency: this complex consists of two subunit proteins, HSP1 and HSP4, which are defective in HPS types 1 and 4, respectively [134,135]. Patients with this type of BLOC deficiency exhibit the most severe form of OCA and bleeding

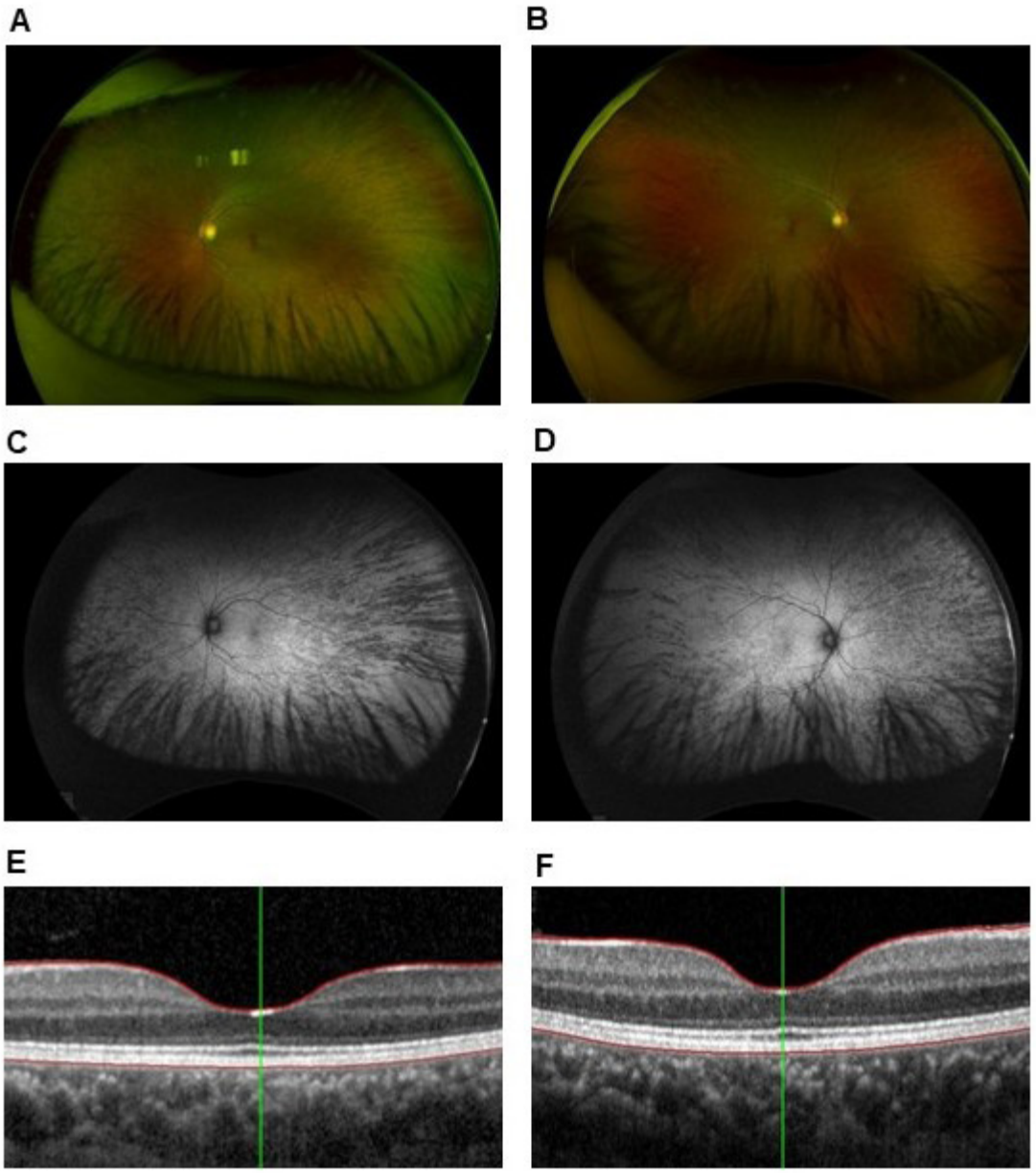

Figure 3. Imaging of a female ocular albinism carrier with confirmed genetic testing (GPR143 variant). Fundus images are captured using Optos ultra-widefield color imaging in the patient's left (**A**) and right (**B**) eyes. Fundus autofluorescence imaging in the patient's left (**C**) and right (**D**) eyes, showing abnormal pigmentary streaks in the peripheral retina. Optical coherence tomography imaging in the patient's left (**E**) and right (**F**) eyes, showing partial foveal hypoplasia. A shallow pit is seen, with the absence of the expansion of the outer nuclear layer seen in normal fovea. The green line indicates where the foveal thickness was measured (the left eye was 185 µm thick and the right eye was 182 µm thick. The normal thickness of the fovea is ≥210 µm).

diathesis. In addition, patients experience a progressive form of lethal pulmonary fibrosis and often receive a lung transplant [136]. AP-3 deficiency: this complex consists of two subunit proteins, AP3B1 and AP3D1, that are defective in HPS types 2 and 10, respectively [137,138]. In addition to OCA, patients exhibit immunodeficiency with increased susceptibility to infection caused by neutropenia. Furthermore, in HSP type 10, additional sensorineural hearing loss and neurodevelopmental delay are present. Based on this genotype-phenotype correlation, early genetic diagnosis

is recommended to determine the most beneficial clinical management.

Chediak-Higashi syndrome: A single locus has been reported for Chediak-Higashi syndrome (CHS), which is a rare autosomal recessive condition characterized by variable OCA, severe immune deficiency, mild bleeding tendency, and neurologic manifestations, including cerebellar ataxia and peripheral neuropathy [139]. The defective gene is a lysosomal trafficking regulator gene (*LYST*) that not only regulates lysosomal trafficking [140] but also is responsible for the synthesis and transport of cytoplasmic granules [141]. Approximately 500 independent cases have been reported that can be classified into three phenotypes: (1) nonsense and frameshift variants are associated with classical, severe CHS; (2) missense variants can be associated with classical or atypical CHS, with milder, late-onset neurologic symptoms; and (3) large deletions and insertions can range from mild to severe CHS, depending on how much of the gene is disrupted [142]. Abnormalities in *LYST* result in abnormally large melanosomes, which impair melanin transfer in melanocytes, causing the variable OCA phenotype with grade 1 FH.

Achromatopsia: Six autosomal recessive achromatopsia loci exhibit an atypical form of FH (Table 1). All of the genes are photoreceptor-specific genes (*CNGA3*, *CNGB3*, *GNAT2*, *PDE6C*, *PDE6H*), except *ATF6*, which encodes a transcription factor regulating the unfolded protein response during endoplasmic reticulum stress [143]. The OCT imaging results in these patients show retention of inner retinal layers with disruption of the ellipsoid hyperreflective layer, which is associated with cone photoreceptor degeneration [10,14]. From a clinical perspective, the visual acuity in this group of patients is significantly worse than any of the other grades of FH [14].

Isolated foveal hypoplasia: Two genes are associated with cases of isolated FH (Table 1). Thus far, 60 disease-causing variants in the solute carrier family 38, member 8 gene (*SLC38A8*) have been found in patients with South Asian, East Asian, Northern European, and Arab ancestry [144]. Although the phenotype typically includes nystagmus, many cases of optic chiasm misrouting have now been recorded, but without the pigmentary deficits of albinism (FHONDA). SLC38A8 is a sodium-dependent glutamine transporter expressed in the brain and retina. Expression studies in cone-enriched retinal organoids suggest SLC38A8 could be involved in foveal development [145]. Since there are no pigmentary abnormalities, it has been suggested that SLC38A8 is downstream of the albinism genes [146].

The second gene causing isolated FH is the aryl hydrocarbon receptor gene (*AHR*), where only three variants have been described in patients of Middle Eastern and North African ancestry [3,147]. FH is grade 3 or 4 in these cases. AHR is a ligand-activated transcription factor involved in immunity and neurogenesis. Targeted deletion of the *Ahr* gene in mice affects optic nerve myelin sheath formation and horizontal eye movement abnormalities [148]. During retinal development in mice, *Ahr* is expressed in developing ganglion cells, so it may be involved in determining the location of the incipient fovea in humans. The exact role of AHR in foveal development warrants testing in a model system.

Developmental abnormalities with foveal hypoplasia: Mutations in 11 genes (paired box 6 [*PAX6*], solute carrier family 25 member 9 [*SLC25A19*], ferm domain-containing protein 7 [*FRMD7*], calcium channel voltage-dependent alpha-1F subunit [*CACNA1F*], NF-kappa-B essential modulator [*NEMO*], frizzle class receptor 4 [*FZD4*], kinesin family member 11 [*KIF11*], tetraspanin 12 [*TSPAN12*], low density lipoprotein receptor-related protein 5 [*LRP5*], norrin cystine knot growth factor [*NDP*], growth differentiation factor 3 [*GDF3*]) are associated with FH present at birth or in the first few months of life (Table 1). The most common of these is infantile nystagmus (prevalence 2.4 per 1,000), which is either idiopathic or accompanying other diseases such as aniridia, albinism, and achromatopsia. Approximately 25% of patients with infantile nystagmus who have disease-causing variants in the *FRMD7* gene have a decrease in foveal pit depth, retained inner nuclear layers, and decreased cone outer segment length [12]. In addition to this grade 1 FH, patients have mild visual acuity deficits and optic nerve hypoplasia. It is not clear why nystagmus occurs, but it could be associated with chiasmal axonal misrouting, a defect in cone photoreceptor cell development, or smooth pursuit system abnormalities [149].

In approximately 80% of cases of aniridia syndrome (prevalence 1:70,000), varying grades of FH are reported [8]. The disease is caused by variants in the *PAX6* gene, which result in haploinsufficiency of the PAX6 transcription factor [150]. To date, 197 unique variants have been reported (LOVD), although this does not include unique mutations in regulatory elements or chromosomal defects [151].

Aland Island eye disease (AIED) [152] and incontinentia pigmenti [153] both exhibit hypopigmentation defects, but without the axonal misrouting deficits seen in typical albinism. AIED is a calcium transport channelopathy due to mutations in the *CACNA1F* gene, and it is allelic with congenital stationary night blindness (CSNB2A) and X-linked cone-rod dystrophy (CORDX3). Mutations in *CACNA1F* cause loss of neurotransmission between photoreceptor cells and bipolar cells and cone-rod dystrophy. The few patients with

AIED who have been examined exhibit grade 3 FH, which is not a feature of CSNB2A, and occurs rarely in CORDX3. Incontinentia pigmenti is an X-linked ectodermal dysplasia with foveal deficits in approximately 35% of patients, which includes the absence of a foveal pit and blood vessels crossing into the FAZ [11,154]. With a prevalence of approximately 1:100,000, disease-causing variants in *IKBKG/NEMO* result in a decrease in activity of the nuclear factor–κB pathway involved in cell death. How *CACNA1F* and *IKBKG/NEMO* genes are involved in foveal development awaits further testing.

FEVR is caused by mutations in five genes (*FZD4*, *KIF11*, *TSPAN12*, *LRP5*, *NDP*). In a comprehensive study, 25% of FEVR cases exhibited grade 1 bilateral FH and 47% unilateral FH [155]. The incidence of FH for each genotype was different, occurring in 100% of *KIF11* cases, 59.3% of *LRP5* cases, and 42.9%, 40%, and 38.2% of *NDP*, *TSPAN12*, and *FZD4* cases, respectively. FEVR affects normal retinal angiogenesis, with NDP, FZD5, and LRP5 forming a complex that activates the β-catenin signaling pathway during development. Therefore, these genes could play a role in the developing FAZ.

Recently, atypical FH has been described in Best's disease [13]. Approximately 27% of patients exhibited FH with a shallow foveal pit, persistence of the inner retinal layers, and blood vessels starting to cross the FAZ. The BEST1 protein oligomerizes to form a BEST1 chloride channel, and a mutant protein may lead to protein mislocalization in the endoplasmic reticulum of RPE cells. The expression of BEST1 and its role during foveal development require further investigation. Mutations in *LAMB2* [156], *SLC25A19* [157], and *GDF3/GDF6* [158] are all associated with rare cases of FH as a feature of other congenital diseases. Whether FH is a consistent feature of these diseases is unclear.

Genetic pathways leading to foveal hypoplasia: Based on the genes involved in FH, several disease mechanisms can be proposed. For instance, mutation of many different genes involved in pigment biogenesis leads to FH, but how these defects occurring in the RPE cause foveal hypoplasia in the adjacent retina has remained an open question.

It has been long established that the RPE plays a critical role in retinal homeostasis, providing growth, trophic, and survival factors during early development; morphogenesis; and a maintenance role in the adult retina. It has been shown that the Pax6 protein cooperates with Mitf to transactivate *Tyr* and *Tyrp1* in RPE cells [159], suggesting that the RPE may have a role in foveal morphogenesis through downstream effectors (Figure 4). TYR is required to produce L-DOPA, leading to eumelanin production through several intermediate steps [146]. TYRP1 stabilizes TYR during this process and, in addition, is required to convert 5,6-dihydroxyindole-2-carboxylic acid to eumelanin. Through a feedback loop, secreted L-DOPA binds to GPR143, resulting in the apical secretion of PEDF [160] and the inhibition of basal VEGF release (a known angiogenesis stimulant). Thus, either the lack of L-DOPA (due to mutations in TYR/TYRP1) or the inability of L-DOPA to activate mutant GPR143 results in reduced PEDF secretion into the interphotoreceptor matrix. PEDF plays a role in photoreceptor neurogenesis, ganglion cell survival, cone opsin synthesis, and the inhibition of angiogenesis [161], which are all key components of foveal morphogenesis. Importantly, in a *Xenopus laevis* model of retinal dysmorphogenesis, PEDF was effective in preserving the development, spatial organization, and morphology of photoreceptors and maintained steady-state levels of opsin after RPE detachment, supporting the notion that RPE-derived PEDF is actively involved in retinal homeostasis [162]. PEDF is a 50-kDa glycoprotein that is synthesized in RPE early in human development (~17 weeks' gestation) [163], positioning its expression at around the time of foveal development. Localization of PEDF to the incipient foveal region in fetal macaque retina [64] suggests it may have an important role in preventing blood vessel formation in the developing FAZ. Based on structure-function relationships, a specific 17–amino acid region defines its neurotrophic action, which interacts with a PEDF receptor (encoded by the *PNPLA2* gene) that localizes to photoreceptor inner segments [164]. Thus, we can propose that PEDF is a crucial signal downstream of the pigment biogenesis pathway involved in foveal morphogenesis.

A second well-characterized pathway involves the genes causing Hermansky-Pudlak syndrome. As described above, four multi-subunit protein complexes (BLOC-1, BLOC-2, BLOC-3, and AP-3) are responsible for the formation and maturation of melanosomes (Figure 5). Defects in melanosome formation or abnormal trafficking contribute to the disease features of HSP. Specifically, how these defects cause foveal hypoplasia remains to be determined. Based on evidence from *GPR143* mutation data in ocular albinism, it is suggested that GPR143 is a biosensor, providing regulatory feedback that controls the size and number of melanosomes [165] by regulating the expression levels of MITF [166]. Thus, it is possible that the genes affected in HPS are connected to the expression of pigment biosynthesis genes downstream of MITF, thereby connecting the two pathways.

Animal models: Surprisingly little is known about how each of the FH disease genes contributes to normal foveal development due to a lack of human tissue analysis and

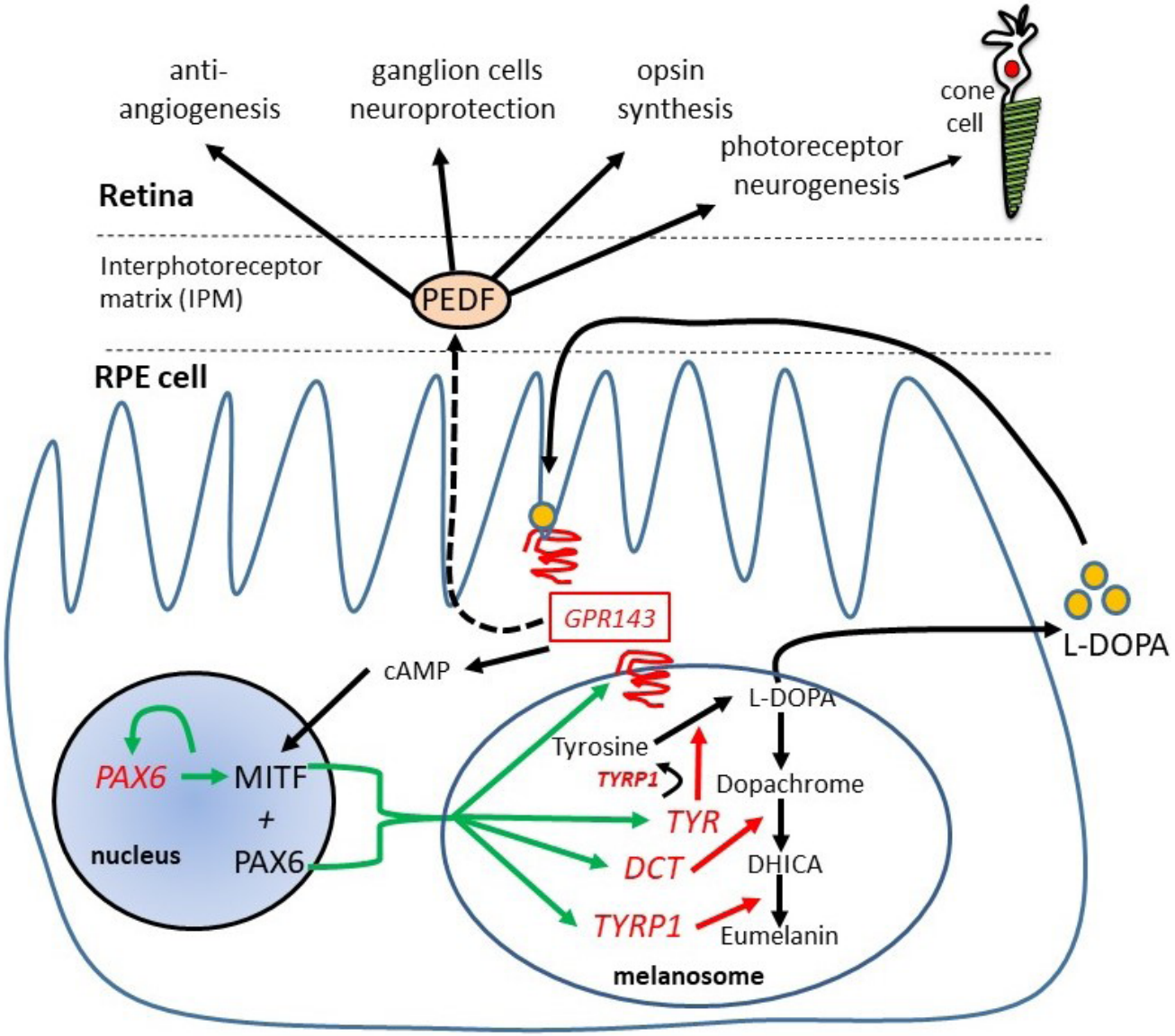

Figure 4. A diagram representing the pigment biogenesis pathway in retinal pigment epithelium (RPE) cells. Mutations in genes that cause foveal hypoplasia are in denoted in red font. The nuclear MITF/PAX6 transcription factors directly regulate the downstream expression of *TYR, TYRP1, DCT*, and *GPR143* genes. The red arrows show which part of the melanin pathway are affected by gene mutations in the melanosome. Some L-DOPA is secreted from the RPE cell and binds to the GPR143 receptor in the RPE membrane, resulting in pigment epithelial-derived factor (PEDF) secretion into the interphotoreceptor matrix. The GPR143 receptor is localized to both the RPE and melanosome membranes. PEDF binds to receptors on ganglion and photoreceptor cells in the retina, eliciting several neurodevelopmental processes including ganglion cell protection, photoreceptor neurogenesis, opsin synthesis and antiangiogenesis pathways.

suitable model system availability. Primate models have been instructive, but they are expensive to use and do not provide enough embryos to be used as a functional model system. Routinely used laboratory models, such as rodents, pigs, dogs, and zebrafish, do not have a fovea structure, but some models (e.g., cats and chickens) have an *area centralis*, where there is an accumulation of cones, photoreceptors, and retinal ganglion cells [167,168]. High visual acuity is critical to the survival of many vertebrate species that are predators and capture live prey primarily through visual guidance. Animal species with a foveal pit include albatross, raptors, pigeons [169-171], seahorses and pipefish [172], and some reptiles [173,174]. However, most of these do not have a fully curated genome, are more difficult to breed, or are considered endangered species. Of the reptile species, the anole lizard is suitable for laboratory study because lizards are

easy to maintain and breed in captivity [175,176], are not an endangered species, and lay eggs before the fovea develops. In addition, the initial genome sequence [177] has now been reannotated to a deep transcriptome level [178].

Anole lizards—anatomy: The diurnal green anole (*Anolis carolinensis*) is an arboreal lizard that lays eggs before foveal formation. The eggs develop rapidly over a period of 22 to 27 days with 19 defined developmental stages [179]. Therefore, to determine the validity of this model system for studying foveal biology, we previously tracked foveal morphogenesis in this species [180]. The anole retina is bifoveated [181] with a central convexiclivate fovea that is thought to provide high visual acuity function [182], while the temporal, shallow fovea plays an important role in depth perception for prey-capture roles [183]. Similar to the human fovea, there is GCL thickening at the position of the presumptive pit at embryonic stage (ES) 10 before pit formation (Figure 6). The foveal pit starts to form at ES17, with thickening of the ONL, and continues to develop after hatching. A yellow pigment underlying the central foveal retinal region, similar to the macular pigment in humans (lutein), is present, which blocks blue light from causing oxidative damage [184]. Structurally, the anole fovea differs from the human fovea in that it has a thicker nerve fiber layer, and there are no nuclei in the ONL at the center of the pit (foveola)—a functional improvement that allows more light to directly access the photoreceptors. The brown anole lizard (*Anolis sagrei*) has also been recently characterized in detail as a model to study foveal development [176,185].

Anole lizards—gene expression studies: For the lizard model to be valuable to study molecular events during foveal development, some of the same genes would need to be expressed in both human and anole tissues. Previous literature reviews of candidate genes that might be involved in foveal/macular development identified a list of 98 genes, of which 86% had orthologous protein sequence matches to the Anolis genome [180]. These candidate genes were identified by several differential expression analysis studies or were known disease genes, suggesting similar molecular pathways between humans and anoles may be active. The expression of two candidate genes (Pax6 and Pedf) has been examined in the developing lizard fovea to test this notion. Pax6 protein expression was first detected at ES14 throughout the retina,

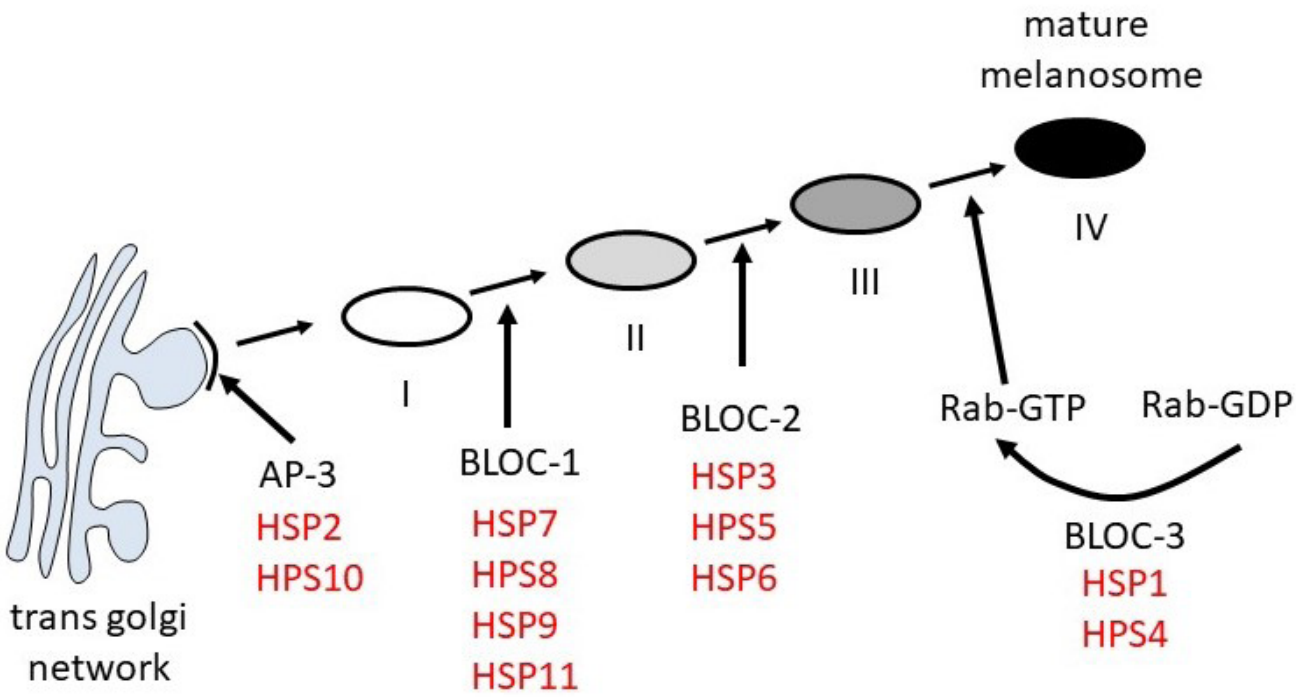

Figure 5. A diagram depicting the biogenesis of melanosomes and protein complexes involved in Hermansky-Pudlak syndrome (HPS). The four stages of melanosome maturation (I-IV) are regulated by four protein complexes (AP-3, BLOC-1, BLOC-2, and BLOC-3). Each protein complex has between 2 and 4 subunit components. When these subunit components are mutated, they result in HPS. BLOC-3 is required for activation of Rabs through conversion of GDP to GTP in the final step of melanosome maturation. The location of the 11 HPS loci in the four protein complexes are indicated in red text.

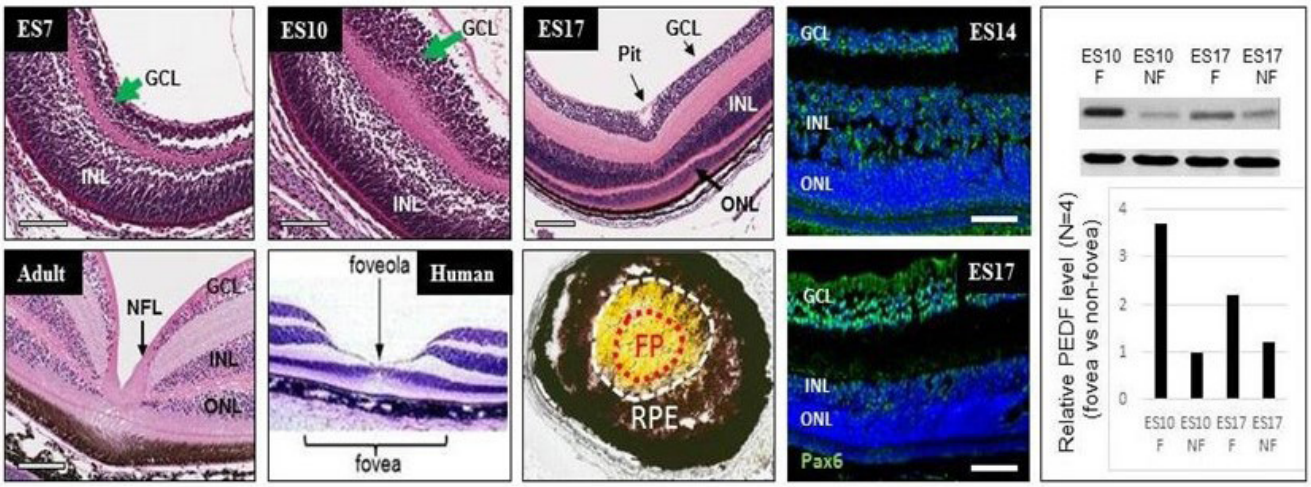

Figure 6. Characteristics of foveal development in the anole retina. Comparison of the embryonic stage (ES) panels ES7 and ES10 (top row) show that at ES10, the ganglion cell layer (GCL) is thickened (green arrow) compared to the retina at embryonic stage ES7. INL, inner nuclear layer (size bar = 50 µm). The start of foveal pit formation is shown in the ES17 panel (arrow), where the fovea has a thickened outer nuclear layer (ONL), compared to a one cell thick ONL at ES10. Comparing the adult and human panels (bottom row), the adult anole fovea has a thick nerve fiber layer (NFL), and there are no nuclei in the ONL in the center of the fovea (size bar = 100 µm) compared to the human foveola, where cells in the ONL are present. When the retina is removed from the posterior anole eye cup, a yellow pigment is revealed (bottom row, third image). The red dotted line shows where the foveal pit (FP) would be positioned, and the yellow pigment extends beyond the FP (white dotted line). The immunochemistry images on the top and bottom rows show that Pax6 protein expression (green) is highest at ES17 in the GCL and at lower levels in the INL compared to ES14 (size bar = 100 µm). The retinal sections are counterstained with Hoechst dye to identify the three nuclear layers. The far-right panel is a Western blot with quantification of signal intensity plot below, showing a nearly three-fold increase in pigment epithelial-derived factor (PEDF) in foveal (F) retina at ES10 compared to non-foveal (NF) retina ($p < 0.001$, $n = 4$), which is not significantly elevated at ES17. Loading control is GAPDH.

but the highest levels of Pax6 expression were observed in the GCL at ES17 (Figure 6). Since PEDF is a downstream target of the pigment pathway genes involved in FH, its expression was tested in anole tissue, revealing Pedf protein was threefold higher in foveal versus nonfoveal tissue at ES10 (Figure 6). This suggests that Pedf may be a crucial signaling molecule that could, for instance, mark the future location of the incipient fovea. Now, many more candidate genes can be tested in this model system by either gene expression analysis or protein localization, assuming that suitable antibodies are available.

Anole lizards—functional testing: For a model system to be valuable, functional testing modalities need to be available to, for instance, standardize the evaluation of genetic manipulations or test potential treatment options. For example, to study the function of the central fovea, we used laser burns to damage the pigmented choroid of the anole eye that provides support to the retina. This resulted in foveal tearing, seen 1 month after laser injury (Figure 7A,B). Lizards were then tested using two functional modalities. Using optokinetic tracking of head movements, a behavioral response mediated through retina-brain circuitry that approximates a measurement of visual acuity [186,187], a 60% reduction in spatial threshold frequency was observed (Figure 7C). Second, a standardized bait-capture test (Figure 7D) was used, where anoles are fasted for specific lengths of time before being offered a live cricket to eat [188]. After 5 days of fasting, eight of eight wild-type controls caught the bait, whereas only three of eight laser-injured anoles were able to catch the bait (Figure 7E). These studies show that the central fovea is required for high-acuity vision.

As seen in human studies, noninvasive OCT has been particularly important in the visualization of retinal pathologies. Therefore, we wondered whether this could be possible in anoles. We used a Pheonix-Micron image-guided OCT2 system to take images in an anesthetized anole. The segmentation of retinal layers we observed matched well with the histology (Figure 8). This OCT imaging could therefore be used in testing genetic manipulation of the anole genome.

Anole lizards—genetic manipulation: One aspect of the anole model that has been challenging is genetic manipulation. Female anoles retain sperm, and the oocytes are fertilized

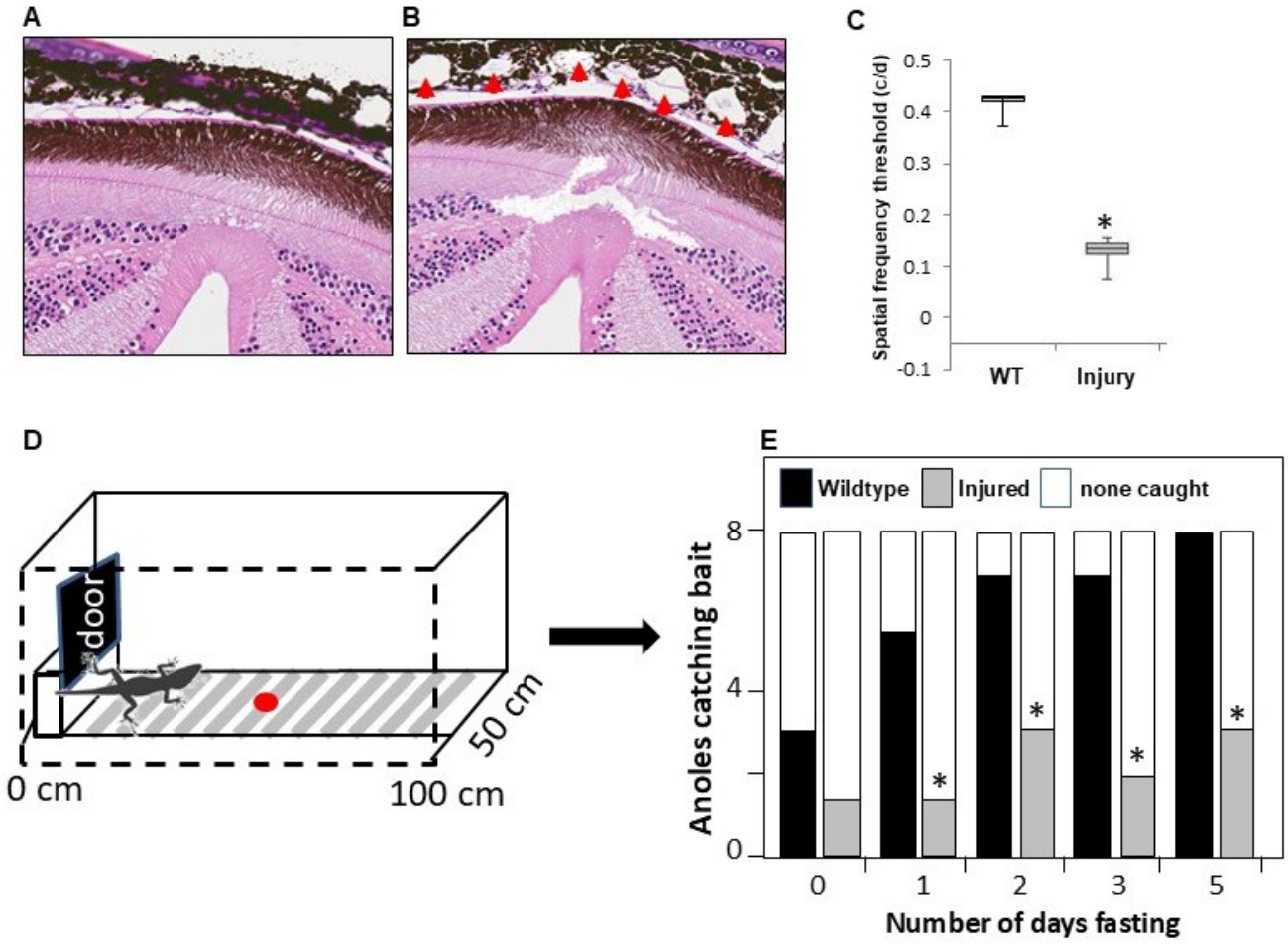

Figure 7. Examples of functional testing in the anole lizard. **A**: This image shows an histological section through the normal fovea structure. **B**: An histological section through an anole retina one month after laser burn injury to the choroid beneath the fovea (red arrowheads). **C**: Optokinetic tracking comparing wild-type anoles to those with laser injury, showing a significant decrease in the spatial frequency threshold (*p<0.001, n=5). **D**: Live bait capture setup where an anole is kept behind a door in a Perspex box and then given access to a single cricket to capture (red dot). Groups of 8 anoles were fasted for between 1 and 5 days, and the number of crickets captured is recorded in the bar chart (**E**). By 5 days of fasting, all 8 wild-type anoles (black bars) caught the bait, but the injured anoles (grey bars) captured significantly less bait (*p < 0.05, n = 8). The white bars indicated how many of the 8 anoles in the test did not catch the bait.

in the oviduct, making injection into single-cell embryos problematic. However, work from two other groups recently showed that CRISPR/Cas9 gene editing in the anole and gecko lizard was achieved, removing this barrier to success [189,190]. Here, a surgical approach was pioneered by Doug Menke and colleagues to inject CRISPR reagents into unfertilized oocytes in the ovaries. After 7 days of recovery, the females were reintroduced to males, and the injected oocytes were fertilized and then laid 3 to 4 weeks postinjection. The *Tyr* gene was targeted to measure the efficiency of genome editing, as the resultant phenotype would be the loss of pigmentation. Interestingly, using three guide RNAs, biallelic knockout lizards were identified in the F0 generation. Subsequent analysis of the eyes from *Tyr*-targeted anole mutants revealed that the central fovea was present, but they had lost the temporal fovea, which was an unexpected finding [191]. More recent observations in knocking down the *Oca2* gene in lizards also caused a loss of the temporal fovea [192]. To complement this work, wild-type lizards were exposed to N-phenylthiourea, an inhibitor of tyrosinase, which caused loss of the central fovea. Most recently, this group has targeted the *ATF6* gene, which causes achromatopsia type 7 [143] by affecting outer segment development and consequent defects in the ellipsoid zone on OCT imaging of the fovea. Targeting of the *Atf6* gene in lizards resulted in the absence of cone outer segments [193]. These gene targeting experiments have

provided proof-of-principle that the anole lizard could be an excellent model to study the foveal development mechanism, but functional characterization of these knockouts needs to be validated.

Treatment for foveal hypoplasia: Due to the timeline for normal foveal development, diseases exhibiting foveal hypoplasia are currently untreatable. However, since foveal development continues after birth in humans, there is a potential therapeutic window during the first few years of life. An interesting approach toward treating albinism was proposed by Glen Jeffrey and colleagues in mice with targeted deletion of the *Tyr* gene, resulting in an underdeveloped retina and chiasmal misrouting [194]. Transgenic expression of tyrosine hydroxylase (which can catalyze the conversion of L-tyrosine to L-DOPA) in the RPE on a *Tyr*-deficient mouse background rescues the retinal abnormalities and visual function, despite the absence of melanin synthesis [195]. This suggests that a lack of L-DOPA or one of its metabolic derivatives is key to the abnormal retinal development and function seen in albinism. Therefore, one possible intervention that has been tested in a clinical trial is oral L-DOPA supplementation [196]. However, albinism patients treated with L-DOPA did not have any improvement in visual acuity. This may be related to the patients aged 3 to 60 years who were treated, which falls outside the critical window of postnatal foveal maturation and retinal plasticity [21,48,197]. To further test the validity of whether postnatal retinal development and visual function can be modulated, *Tyr*-deficient mice have been administered oral L-DOPA in the early stages of life by Helena Lee and colleagues [198,199]. Compared to untreated mice, those treated from birth or from weaning for 28 days with L-DOPA had improved packing density of photoreceptors in the ONL, normalized a- and b-wave amplitudes on electroretinography testing, and improved spatial frequency thresholds on optokinetic tracking (OKT) testing measuring visual acuity. Interestingly, treatment with L-DOPA showed a dose-dependent increase in PEDF levels in *Tyr*-deficient mouse eyes. These data suggest that a clinical trial of L-DOPA in albinism infants is warranted. Although mice do not have a fovea, the rescue of the morphological and function defects during postnatal treatment suggests that this could be tested in the *Tyr* anole CRISPR model to see if the absence of the temporal fovea can be rescued.

A second approach to treat *GPR143*-related albinism has been to develop antisense oligonucleotides (AONs) to block aberrant retention of an intron caused by the mutation, creating a new splice site acceptor [105]. Using melanocytes cultured from patient biopsy specimens, the AON was able to restore GPR143 expression that underwent posttranslational glycosylation. AONs are being tested in a wide range of ophthalmic conditions [200], as well as to inhibit the growth of aberrant blood vessels that may be applicable to FAZ defects [201]. These types of approaches may be relevant to FH if they can be administered during the window of neurologic plasticity in the first few years of life [197].

Based on knowledge gained from understanding how L-DOPA and PEDF inhibit angiogenesis to support normal development of the FAZ, clinical trials of L-DOPA for inhibiting foveal angiogenesis in AMD have been performed. One study showed that patients being treated with L-DOPA had a 21% to 35% reduction of conversion to neovascular AMD [202], and in a second study, L-DOPA treatment was correlated with a 32% reduction in new-onset geographic AMD [203]. Similarly, L-DOPA has been tested in mouse models of diabetic retinopathy and found to have a neuroprotective role on ganglion cells [204]. These examples exemplify how

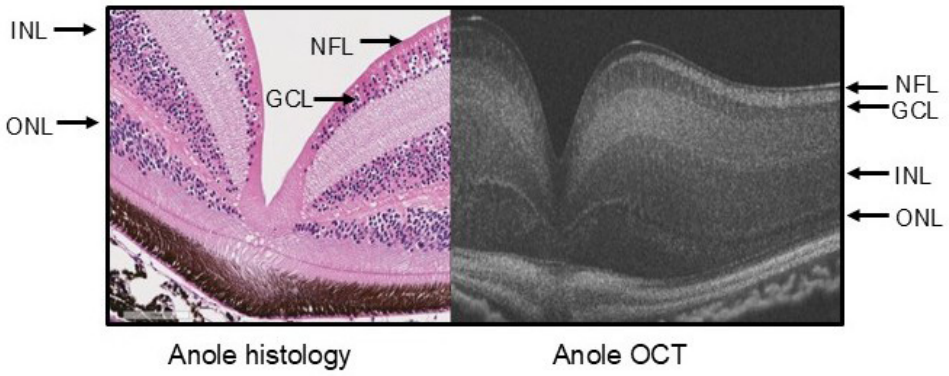

Figure 8. An example of optical coherence tomography (OCT) live imaging of the anole retina. The left image shows a histological section through the anole fovea. The right image shows OCT imaging through the anole eye. The nuclear layers (outer nuclear layer [ONL], inner nuclear layer [INL], and ganglion cell layer [GCL]) and the nerve fiber layer (NFL) in the OCT image line up with the layers in the histology image next to it.

knowledge of foveal developmental mechanisms can have an impact on diseases that affect the adult fovea.

Conclusion: The fovea is critically important to human vision. Now that most genes that cause FH have been identified, a suitable animal model system has been validated, and functional testing is available, this should stimulate fundamental advances in understanding the molecular and cellular mechanisms of foveal maturation and how gene mutation leads to foveal damage. This information is needed to direct interventions to improve foveal maturation and thereby prevent poor vision.

ACKNOWLEDGMENTS

This work was supported by the Sharon Stewart Trust (SST07130414) and Fighting Blindness Canada Patient Registry FBCReg2025). We thank Dr. Kaivon Vaezi, Consultant Ophthalmologist, Eye Care Centre for providing images of OCTA in Figure 1E,F. Figure 2 is adapted from a previous publication by the authors [1]. We also thank Xianghong Shan for OCT imaging of the lizard retina.

REFERENCES

1. Gregory-Evans CY, Gregory-Evans K. Foveal hypoplasia: the case for arrested development. Expert Rev Ophthalmol 2011; 6:565-74. .
2. Querques G, Prascina F, Iaculli C, Delle Noci N. Isolated foveal hypoplasia. Int Ophthalmol 2009; 29:271-4. [PMID: 18401554].
3. Mayer AK, Mahajnah M, Thomas MG, Cohen Y, Habib A, Schulze M, Maconachie GDE, AlMoallem B, De Baere E, Lorenz B, Traboulsi EI, Kohl S, Azem A, Bauer P, Gottlob I, Sharkia R, Wissinger B. Homozygous stop mutation in AHR causes autosomal recessive foveal hypoplasia and infantile nystagmus. Brain 2019; 142:1528-34. [PMID: 31009037].
4. Perez Y, Gradstein L, Flusser H, Markus B, Cohen I, Langer Y, Marcus M, Lifshitz T, Kadir R, Birk OS. Isolated foveal hypoplasia with secondary nystagmus and low vision is associated with a homozygous SLC38A8 mutation. Eur J Hum Genet 2014; 22:703-6. [PMID: 24045842].
5. Oetting WS, King RA. Molecular basis of albinism: mutations and polymorphisms of pigmentation genes associated with albinism. Hum Mutat 1999; 13:99-115. [PMID: 10094567].
6. Recchia FM, Recchia CC. Foveal dysplasia evident by optical coherence tomography in patients with a history of retinopathy of prematurity. Retina 2007; 27:1221-6. [PMID: 18046228].
7. Gregory-Evans K, Cheong-Leen R, George SM, Xie J, Moosajee M, Colapinto P, Gregory-Evans CY. Non-invasive anterior segment and posterior segment optical coherence tomography and phenotypic characterization of aniridia. Can J Ophthalmol 2011; 46:337-44. [PMID: 21816254].
8. Sannan NS, Gregory-Evans CY, Lyons CJ, Lehman AM, Langlois S, Warner SJ, Zakrzewski H, Gregory-Evans K. Correlation of novel PAX6 gene abnormalities in aniridia and clinical presentation. Can J Ophthalmol 2017; 52:570-7. [PMID: 29217025].
9. Dentel A, Ferrari M, Robert MP, Valleix S, Bremond-Gignac D, Daruich A. Optical coherence tomography angiography assessment in congenital aniridia. Am J Ophthalmol 2023; 253:44-8. [PMID: 37059316].
10. Thomas MG, Kumar A, Kohl S, Proudlock FA, Gottlob I. High-resolution in vivo imaging in achromatopsia. Ophthalmology 2011; 118:882-7. [PMID: 21211844].
11. Goldberg MF, Custis PH. Retinal and other manifestations of incontinentia pigmenti (Bloch-Sulzberger syndrome). Ophthalmology 1993; 100:1645-54. [PMID: 8233390].
12. Tarpey P, Thomas S, Sarvananthan N, Mallya U, Lisgo S, Talbot CJ, Roberts EO, Awan M, Surendran M, McLean RJ, Reinecke RD, Langmann A, Lindner S, Koch M, Jain S, Woodruff G, Gale RP, Bastawrous A, Degg C, Droutsas K, Asproudis I, Zubcov AA, Pieh C, Veal CD, Machado RD, Backhouse OC, Baumber L, Constantinescu CS, Brodsky MC, Hunter DG, Hertle RW, Read RJ, Edkins S, O'Meara S, Parker A, Stevens C, Teague J, Wooster R, Futreal PA, Trembath RC, Stratton MR, Raymond FL, Gottlob I. Mutations in FRMD7, a newly identified member of the FERM family, cause X-linked idiopathic congenital nystagmus. Nat Genet 2006; 38:1242-4. [PMID: 17013395].
13. Moret E, Lejoyeux R, Bonnin S, Azar G, Guillaume J, Le Cossec C, Lafolie J, Alonso A-S, Favard C, Meunier I, Vasseur V, Mauget-Faÿsse M. Atypical foveal hypoplasia in Best disease. J Pers Med 2023; 13:337-[PMID: 36836571].
14. Kuht HJ, Maconachie GDE, Han J, Kessel L, van Genderen MM, McLean RJ, Hisaund M, Tu Z, Hertle RW, Gronskov K, Bai D, Wei A, Li W, Jiao Y, Smirnov V, Choi J-H, Tobin MD, Sheth V, Purohit R, Dawar B, Girach A, Strul S, May L, Chen FK, Heath Jeffery RC, Aamir A, Sano R, Jin J, Brooks BP, Kohl S, Arveiler B, Montoliu L, Engle EC, Proudlock FA, Nishad G, Pani P, Varma G, Gottlob I, Thomas MG. Genotypic and phenotypic spectrum of foveal hypoplasia. A multicenter study. Ophthalmology 2022; 129:708-18. [PMID: 35157951].
15. Daruich A, Robert MP, Leroy C, DE Vergnes N, Beugnet C, Malan V, Valleix S, Bremond-Gignac D. Aniridia: Correlation to phenotype and PAX6 genotype. Am J Ophthalmol 2022; 237:122-9. [PMID: 34942114].
16. Netland PA, Scott ML, Boyle JW 4th, Lauderdale JD. Ocular and systemic findings in a survey of aniridia subjects. J AAPOS 2011; 15:562-6. [PMID: 22153401].
17. Li J, Tso MO, Lam TT. Reduced amplitude and delayed latency in foveal response of multifocal electroretinogram in early age related macular degeneration. Br J Ophthalmol 2001; 85:287-90. [PMID: 11222332].
18. Kim K, Kim ES, Yu SY. Optical coherence tomography angiography analysis of foveal microvascular changes and

inner retinal layer thinning in patients with diabetes. Br J Ophthalmol 2018; 102:1226-31. [PMID: 29259019].

19. Bloom DE, Cafiero ET, Jané-Llopis E, Abrahams-Gessel S, Bloom LR, Fathima S, Feigl AB, Gaziano T, Mowafi M, Pandya A, Prettner K, Rosenberg L, Seligman B, Stein AZ, Weinstein C. (2011) The Global Economic Burden of Noncommunicable Diseases. Geneva: World Economic Forum. WEF_Harvard_HE_GlobalEconomicBurdenNonCommunicableDiseases_2011.pdf

20. Paudel N, Brady L, Stratieva P, Galvin O, Lui B, Van den Brande I, Malkowski J-P, Rebeira M, MacAllister S, O'Riordan T, Daly A. Economic burden of late-stage age-related macular degeneration in Bulgaria, Germany and the US. JAMA Ophthalmol 2024; 142:1123-30. The impact of AMD on Germany, Bulgaria and the USA[PMID: 39480444].

21. Hendrickson AE, Yuodelis C. The morphological development of the human fovea. Ophthalmology 1984; 91:603-12. [PMID: 6462623].

22. Provis JM, Hendrickson AE. The foveal avascular region of developing human retina. Arch Ophthalmol 2008; 126:507-11. [PMID: 18413520].

23. Azzopardi P, Cowey A. Preferential representation of the fovea in the primary visual cortex. Nature 1993; 361:719-21. [PMID: 7680108].

24. Hendrickson AE. Primate foveal development: a microcosm of current questions in neurobiology. Invest Ophthalmol Vis Sci 1994; 35:3129-33. [PMID: 8045707].

25. Bumsted K, Hendrickson A. Distribution and development of short-wavelength cones differ between Macaca monkey and human fovea. J Comp Neurol 1999; 403:502-16. [PMID: 9888315].

26. Castaño JA, Sperling HG. Sensitivity of the blue-sensitive cones across the central retina. Vision Res 1982; 22:661-73. [PMID: 7112960].

27. Recchia FM, Carvalho-Recchia CA, Trese MT. Optical coherence tomography in the diagnosis of foveal hypoplasia. Arch Ophthalmol 2002; 120:1587-8. [PMID: 12427081].

28. McGuire DE, Weinreb RN, Goldbaum MH. Foveal hypoplasia demonstrated in vivo with optical coherence tomography. Am J Ophthalmol 2003; 135:112-4. [PMID: 12504716].

29. Seo JH, Yu YS, Kim JH, Choung HK, Heo JW, Kim SJ. Correlation of visual acuity with foveal hypoplasia grading by optical coherence tomography in albinism. Ophthalmology 2007; 114:1547-51. [PMID: 17337060].

30. Cronin TH, Hertle RW, Ishikawa H, Schuman JS. Spectral domain optical coherence tomography for detection of foveal morphology in patients with nystagmus. J AAPOS 2009; 13:563-6. [PMID: 20006817].

31. Thomas MG, Kumar A, Mohammad S, Proudlock FA, Engle EC, Andrews C, Chan W-M, Thomas S, Gottlob I. Structural grading of foveal hypoplasia using spectral-domain optical coherence tomography a predictor of visual acuity? Ophthalmology 2011; 118:1653-60. [PMID: 21529956].

32. Marmor MF, Choi SS, Zawadzki RJ, Werner JS. Visual insignificance of the foveal pit: reassessment of foveal hypoplasia as fovea plana. Arch Ophthalmol 2008; 126:907-13. [PMID: 18625935].

33. Wilk MA, McAllister JT, Cooper RF, Dubis AM, Patitucci TN, Summerfelt P, Anderson JL, Stepien KE, Costakos DM, Connor TB Jr, Wirostko WJ, Chiang P-W, Dubra A, Curcio CA, Brilliant MH, Summers CG, Carroll J. Relationship between foveal cone specialization and pit morphology in albinism. Invest Ophthalmol Vis Sci 2014; 55:4186-98. [PMID: 24845642].

34. Lee H, Purohit R, Patel A, Papageorgiou E, Sheth V, Maconachie G, Pilat A, McLean RJ, Proudlock FA, Gottlob I. In vivo foveal development using optical coherence tomography. Invest Ophthalmol Vis Sci 2015; 56:4537-45. [PMID: 26200492].

35. Rufai SR, Thomas MG, Purohit R, Bunce C, Lee H, Proudlock FA, Gottlob I. Can structural grading of foveal hypoplasia predict future vision in infantile nystagmus?: A longitudinal study. Ophthalmology 2020; 127:492-500. [PMID: 31937464].

36. Spaide RF, Klancnik JM Jr, Cooney MJ. Retinal vascular layers imaged by fluorescein angiography and optical coherence tomography angiography. JAMA Ophthalmol 2015; 133:45-50. [PMID: 25317632].

37. Pakzad-Vaezi K, Keane PA, Cardoso JN, Egan C, Tufail A. Optical coherence tomography angiography of foveal hypoplasia. Br J Ophthalmol 2017; 101:985-8. [PMID: 27899366].

38. Yuan M, Romano F, Ding X, Garcia M, Garg I, Overbey KM, Bennett C, Ploumi I, Stettler I, Lains I, Vingopoulos F, Rodriguez J, Patel NA, Kim LA, Vavvas DG, Husain D, Miller JW, Miller JB. Clinical and imaging characteristics associated with foveal neovascularization in proliferative diabetic retinopathy. Graefes Arch Clin Exp Ophthalmol 2025; 263:679-87. [PMID: 39542876].

39. Cao D, Yang D, Huang Z, Zeng Y, Wang J, Hu Y, Zhang L. Optical coherence tomography angiography discerns preclinical diabetic retinopathy in eyes of patients with type 2 diabetes without clinical diabetic retinopathy. Acta Diabetol 2018; 55:469-77. [PMID: 29453673].

40. Aitchison RT, Kennedy GJ, Shu X, Mansfield DC, Kir R, Hui J, Shahani U. Measuring the foveal avascular zone in diabetes: A study using optical coherence tomography angiography. J Diabetes Investig 2022; 13:668-76. [PMID: 34783201].

41. Shin YI, Kim JM, Lee MW, Jo YJ, Kim JY. Characteristics of the foveal microvasculature in asian patients with dry age-related macular degeneration: an optical coherence tomography angiography study. Ophthalmologica 2020; 243:145-53. [PMID: 31645037].

42. Borrelli E, Barresi C, Berni A, Viggiano P, Reibaldi M, Introini U, Bandello F. OCT risk factors for 2-year foveal involvement in non-treated eyes with extrafoveal geographic atrophy and AMD. Graefes Arch Clin Exp Ophthalmol 2024; 262:2101-9. [PMID: 38326629].

43. Trinh M, Tong J, Yoshioka N, Zangerl B, Kalloniatis M, Nivison-Smith L. Macula ganglion cell thickness changes display location-specific variation patterns in intermediate age-related macular degeneration Invest Ophthalmol Vis Sci 2020; 61:2-[PMID: 32150251].

44. Borrelli E, Abdelfattah NS, Uji A, Nittala MG, Boyer DS, Sadda SR. Postreceptor neuronal loss in intermediate age-related macular degeneration. Am J Ophthalmol 2017; 181:1-11. [PMID: 28624323].

45. Mintz-Hittner HA, Knight-Nanan DM, Satriano DR, Kretzer FL. A small foveal avascular zone may be an historic mark of prematurity. Ophthalmology 1999; 106:1409-13. [PMID: 10406630].

46. Yanni SE, Wang J, Chan M, Carroll J, Farsiu S, Leffler JN, Spencer R, Birch EE. Foveal avascular zone and foveal pit formation after preterm birth. Br J Ophthalmol 2012; 96:961-6. [PMID: 22544530].

47. Yuodelis C, Hendrickson A. A qualitative and quantitative analysis of the human fovea during development. Vision Res 1986; 26:847-55. [PMID: 3750868].

48. Hendrickson A. A morphological comparison of foveal development in man and monkey. Eye (Lond) 1992; 6:136-44. [PMID: 1624035].

49. Hendrickson A, Djajadi H, Erickson A, Possin D. Development of the human retina in the absence of ganglion cells. Exp Eye Res 2006; 83:920-31. [PMID: 16793038].

50. Hendrickson A, Zhang C. Development of cone photoreceptors and their synapses in the human and monkey fovea. J Comp Neurol 2019; 527:38-51. [PMID: 28074469].

51. Linberg KA, Fisher SK. A burst of differentiation in the outer posterior retina of the eleven-week human fetus: an ultrastructural study. Vis Neurosci 1990; 5:43-60. [PMID: 2271459].

52. Provis JM, van Driel D, Billson FA, Russell P. Development of the human retina: patterns of cell distribution and redistribution in the ganglion cell layer. J Comp Neurol 1985; 233:429-51. [PMID: 3980779].

53. Provis JM, Sandercoe T, Hendrickson AE. Astrocytes and blood vessels define the foveal rim during primate retinal development. Invest Ophthalmol Vis Sci 2000; 41:2827-36. [PMID: 10967034].

54. Sandercoe TM, Madigan MC, Billson FA, Penfold PL, Provis JM. Astrocyte proliferation during development of the human retinal vasculature. Exp Eye Res 1999; 69:511-23. [PMID: 10548471].

55. Schein SJ. Anatomy of macaque fovea and spatial densities of neurons in foveal representation. J Comp Neurol 1988; 269:479-505. [PMID: 3372725].

56. McDonald MA, Dobson V, Sebris SL, Baitch L, Varner D, Teller DY. The acuity card procedure: a rapid test of infant acuity. Invest Ophthalmol Vis Sci 1985; 26:1158-62. [PMID: 4019107].

57. Provis JM, Dubis AM, Maddess T, Carroll J. Adaptation of the central retina for high acuity vision: cones, the fovea and the avascular zone. Prog Retin Eye Res 2013; 35:63-81. [PMID: 23500068].

58. Oliver MD, Dotan SA, Chemke J, Abraham FA. Isolated foveal hypoplasia. Br J Ophthalmol 1987; 71:926-30. [PMID: 3427001].

59. Provis JM, Leech J, Diaz CM, Penfold PL, Stone J, Keshet E. Development of the human retinal vasculature: cellular relations and VEGF expression. Exp Eye Res 1997; 65:555-68. [PMID: 9464188].

60. Springer AD. New role for the primate fovea: a retinal excavation determines photoreceptor deployment and shape. Vis Neurosci 1999; 16:629-36. [PMID: 10431912].

61. Springer AD, Hendrickson AE. Development of the primate area of high acuity. 1. Use of finite element analysis models to identify mechanical variables affecting pit formation. Vis Neurosci 2004; 21:53-62. [PMID: 15137581].

62. Springer AD, Hendrickson AE. Development of the primate area of high acuity. 2. Quantitative morphological changes associated with retinal and pars plana growth. Vis Neurosci 2004; 21:775-90. [PMID: 15683563].

63. Springer AD, Hendrickson AE. Development of the primate area of high acuity, 3: temporal relationships between pit formation, retinal elongation and cone packing. Vis Neurosci 2005; 22:171-85. [PMID: 15935110].

64. Kozulin P, Natoli R, O'Brien KM, Madigan MC, Provis JM. Differential expression of anti-angiogenic factors and guidance genes in the developing macula. Mol Vis 2009; 15:45-59. [PMID: 19145251].

65. Kozulin P, Natoli R, Bumsted O'Brien KM, Madigan MC, Provis JM. The cellular expression of antiangiogenic factors in fetal primate macula. Invest Ophthalmol Vis Sci 2010; 51:4298-306. [PMID: 20357200].

66. Bernstein SL, Borst DE, Wong PW. Isolation of differentially expressed human fovea genes: candidates for macular disease. Mol Vis 1995; 1:4-[PMID: 9238082].

67. Bernstein SL, Borst DE, Neuder ME, Wong P. Characterization of a human fovea cDNA library and regional differential gene expression in the human retina. Genomics 1996; 32:301-8. [PMID: 8838792].

68. Sharon D, Blackshaw S, Cepko CL, Dryja TP. Profile of the genes expressed in the human peripheral retina, macula, and retinal pigment epithelium determined through serial analysis of gene expression (SAGE). Proc Natl Acad Sci U S A 2002; 99:315-20. [PMID: 11756676].

69. Bowes Rickman C, Ebright JN, Zavodni ZJ, Yu L, Wang T, Daiger SP, Wistow G, Boon K, Hauser MA. Defining the human macula transcriptome and candidate retinal disease genes using EyeSAGE. Invest Ophthalmol Vis Sci 2006; 47:2305-16. [PMID: 16723438].

70. Radeke MJ, Peterson KE, Johnson LV, Anderson DH. Disease susceptibility of the human macula: differential gene transcription in the retinal pigmented epithelium/choroid. Exp Eye Res 2007; 85:366-80. [PMID: 17662275].

71. Whitmore SS, Wagner AH, DeLuca AP, Drack AV, Stone EM, Tucker BA, Zeng S, Braun TA, Mullins RF, Scheetz TE. Transcriptomic analysis across nasal, temporal, and macular regions of human neural retina and RPE/choroid by RNA-Seq. Exp Eye Res 2014; 129:93-106. [PMID: 25446321].

72. Voigt AP, Whitmore SS, Flamme-Wiese MJ, Riker MJ, Wiley LA, Tucker BA, Stone EM, Mullins RF, Scheetz TE. Molecular characterization of foveal versus peripheral human retina by single-cell RNA sequencing. Exp Eye Res 2019; 184:234-42. [PMID: 31075224].

73. Peng YR, Shekhar K, Yan W, Herrmann D, Sappington A, Bryman GS, van Zyl T, Do MTH, Regev A, Sanes JR. Molecular classification and comparative taxonomics of foveal and peripheral cells in primate retina. Cell 2019; 176:1222-1237. e22. [PMID: 30712875].

74. Yan W, Peng Y-R, van Zyl T, Regev A, Shekhar K, Juric D, Sanes JR. Cell atlas of the human fovea and peripheral retina. Sci Rep 2020; 10:9802-[PMID: 32555229].

75. Mungale A, McGaughey DM, Zhang C, Yousaf S, Liu J, Brooks BP, Maminishkis A, Fufa TD, Hufnagel RB. Transcriptional mapping of the macaque retina and RPE-choroid reveals conserved inter-tissue transcription drivers and signaling pathways. Front Genet 2022; 13:949449[PMID: 36506320].

76. Zhang L, Cavallini M, Wang J, Xin R, Zhang Q, Feng G, Sanes JR, Peng Y-R. Evolutionary and developmental specialization of foveal cell types in the marmoset. Proc Natl Acad Sci U S A 2024; 121:e2313820121[PMID: 38598343].

77. Suchting S, Bicknell R, Eichmann A. Neuronal clues to vascular guidance. Exp Cell Res 2006; 312:668-75. [PMID: 16330027].

78. Volpert OV, Zaichuk T, Zhou W, Reiher F, Ferguson TA, Stuart PM, Amin M, Bouck NP. Inducer-stimulated Fas targets activated endothelium for destruction by anti-angiogenic thrombospondin-1 and pigment epithelium-derived factor. Nat Med 2002; 8:349-57. [PMID: 11927940].

79. Ohno-Matsui K, Morita I, Tombran-Tink J, Mrazek D, Onodera M, Uetama T, Hayano M, Murota SI, Mochizuki M. Novel mechanism for age-related macular degeneration: an equilibrium shift between the angiogenesis factors VEGF and PEDF. J Cell Physiol 2001; 189:323-33. [PMID: 11748590].

80. Rollín R, Mediero A, Roldán-Pallarés M, Fernández-Cruz A, Fernández-Durango R. Natriuretic peptide system in the human retina. Mol Vis 2004; 10:15-22. [PMID: 14737067].

81. Jin Y, Zhong YM, Yang XL. Natriuretic peptides are localized to rat retinal amacrine cells. Neurosci Lett 2007; 421:106-9. [PMID: 17566658].

82. Pedram A, Razandi M, Levin ER. Natriuretic peptides suppress vascular endothelial cell growth factor signaling to angiogenesis. Endocrinology 2001; 142:1578-86. [PMID: 11250939].

83. Sarkar H, Moosajee M. Retinol dehydrogenase 12 (RDH12): Role in vision, retinal disease and future perspectives. Exp Eye Res 2019; 188:107793[PMID: 31505163].

84. Jiang L, Yin M, Wei X, Liu J, Wang X, Niu C, Kang X, Xu J, Zhou Z, Sun S, Wang X, Zheng X, Duan S, Yao K, Qian R, Sun N, Chen A, Wang R, Zhang J, Chen S, Meng D. Bach1 represses Wnt/β-catenin signaling and angiogenesis. Circ Res 2015; 117:364-75. [PMID: 26123998].

85. Mayer AK, Mahajnah M, Thomas MG, Cohen Y, Habib A, Schulze M, Maconachie GDE, AlMoallem B, De Baere E, Lorenz B, Traboulsi EI, Kohl S, Azem A, Bauer P, Gottlob I, Sharkia R, Wissinger B. Homozygous stop mutation in AHR causes autosomal recessive foveal hypoplasia and infantile nystagmus. Brain 2019; 142:1528-34. [PMID: 31009037].

86. Chevallier A, Mialot A, Petit JM, Fernandez-Salguero P, Barouki R, Coumoul X, Beraneck M. Oculomotor deficits in aryl hydrocarbon receptor null mouse. PLoS One 2013; 8:e53520[PMID: 23301081].

87. Kuwajima T, Soares CA, Sitko AA, Lefebvre V, Mason C. SoxC transcription factors promote contralateral retinal ganglion cell differentiation and axon guidance in the mouse visual system. Neuron 2017; 93:1110-1125.e5. [PMID: 28215559].

88. Nie S, Li B, Wang M, Chen Z, Ren J, Li Z, Xu X, Qian Z, Xie Z, Han J, Zhang Z, Zhang Z, Zhu Y, Chen Z, Yang X, Ye K. Sox6 and ALDH1A1 truncation by asparagine endopeptidase defines selective vulnerability in Parkinson's Disease. Adv Sci (Weinh) 2025; 12:e2409477[PMID: 39573918].

89. Panman L, Papathanou M, Laguna A, Oosterveen T, Volakakis N, Acampora D, Kurtsdotter I, Yoshitake T, Kehr J, Joodmardi E, Muhr J, Simeone A, Ericson J, Perlmann T. Sox6 and Otx2 control the specification of substantia nigra and ventral tegmental area dopamine neurons. Cell Rep 2014; 8:1018-25. [PMID: 25127144].

90. Rudrabhatla P, Utreras E, Jaffe H, Kulkarni AB. Regulation of Sox6 by cyclin dependent kinase 5 in brain. PLoS One 2014; 9:e89310[PMID: 24662752].

91. Cornish EE, Madigan MC, Natoli R, Hales A, Hendrickson AE, Provis JM. Gradients of cone differentiation and FGF expression during development of the foveal depression in macaque retina. Vis Neurosci 2005; 22:447-59. [PMID: 16212702].

92. Cornish EE, Natoli RC, Hendrickson A, Provis JM. Differential distribution of fibroblast growth factor receptors (FGFRs) on foveal cones: FGFR-4 is an early marker of cone photoreceptors. Mol Vis 2004; 10:1-14. [PMID: 14737068].

93. Romo P, Madigan MC, Provis JM, Cullen KM. Differential effects of TGF-β and FGF-2 on in vitro proliferation and migration of primate retinal endothelial and Müller cells. Acta Ophthalmol 2011; 89:e263-8. [PMID: 20670342].

94. Sandercoe TM, Geller SF, Hendrickson AE, Stone J, Provis JM. VEGF expression by ganglion cells in central retina before formation of the foveal depression in monkey retina: evidence of developmental hypoxia. J Comp Neurol 2003; 462:42-54. [PMID: 12761823].

95. Stone J, Maslim J. Mechanisms of retinal angiogenesis. Prog Retin Eye Res 1997; 16:157-81. .

96. Stone J, Itin A, Alon T, Pe'er J, Gnessin H, Chan-Ling T, Keshet E. Development of retinal vasculature is mediated by hypoxia-induced vascular endothelial growth factor (VEGF) expression by neuroglia. J Neurosci 1995; 15:4738-47. [PMID: 7623107].

97. Jin KL, Mao XO, Greenberg DA. Vascular endothelial growth factor: direct neuroprotective effect in in vitro ischemia. Proc Natl Acad Sci U S A 2000; 97:10242-7. [PMID: 10963684].

98. Böcker-Meffert S, Rosenstiel P, Röhl C, Warneke N, Held-Feindt J, Sievers J, Lucius R. Erythropoietin and VEGF promote neural outgrowth from retinal explants in postnatal rats. Invest Ophthalmol Vis Sci 2002; 43:2021-6. [PMID: 12037014].

99. Mori K, Duh E, Gehlbach P, Ando A, Takahashi K, Pearlman J, Mori K, Yang HS, Zack DJ, Ettyreddy D, Brough DE, Wei LL, Campochiaro PA. Pigment epithelium-derived factor inhibits retinal and choroidal neovascularization. J Cell Physiol 2001; 188:253-63. [PMID: 11424092].

100. Moreno-Artero E, Morice-Picard F, Bremond-Gignac D, Drumare-Bouvet I, Duncombe-Poulet C, Leclerc-Mercier S, Dufresne H, Kaplan J, Jouanne B, Arveiler B, Taieb A, Hadj-Rabia S. Management of albinism: French guidelines for diagnosis and care. J Eur Acad Dermatol Venereol 2021; 35:1449-59. [PMID: 34042219].

101. Bassi MT, Schiaffino MV, Renieri A, De Nigris F, Galli L, Bruttini M, Gebbia M, Bergen AA, Lewis RA, Ballabio A. Cloning of the gene for ocular albinism type 1 from the distal short arm of the X chromosome. Nat Genet 1995; 10:13-9. [PMID: 7647783].

102. De Filippo E, Schiedel AC, Manga P. Interaction between G protein-coupled receptor 143 and tyrosinase: implications for understanding ocular albinism type 1. J Invest Dermatol 2017; 137:457-65. [PMID: 27720922].

103. Kumar CM, Sathisha UV, Dharmesh S, Rao AGA, Singh SA. Interaction of sesamol (3,4-methylenedioxyphenol) with tyrosinase and its effect on melanin synthesis. Biochimie 2011; 93:562-9. [PMID: 21144881].

104. Khan KN, Lord EC, Arno G, Islam F, Carss KJ, Raymond F, Toomes C, Ali M, Inglehearn CF, Webster AR, Moore AT, Poulter JA, Michaelides M. Detailed retinal imaging in carriers of ocular albinism. Retina 2018; 38:620-8. [PMID: 28234808].

105. Vetrini F, Tammaro R, Bondanza S, Surace EM, Auricchio A, De Luca M, Ballabio A, Marigo V. Aberrant splicing in the ocular albinism type 1 gene (OA1/GPR143) is corrected in vitro by morpholino antisense oligonucleotides. Hum Mutat 2006; 27:420-6. [PMID: 16550551].

106. Kromberg JGR, Flynn KA, Kerr RA. Determining a worldwide prevalence of oculocutaneous albinism: a systematic review. Invest Ophthalmol Vis Sci 2023; 64:14-[PMID: 37440261].

107. Lee S-T, Nicholls RD, Bundey S, Laxova R, Musarella M, Spritz RA. Mutations of the P gene in oculocutaneous albinism, ocular albinism, and Prader-Willi syndrome plus albinism. N Engl J Med 1994; 330:529-34. [PMID: 8302318].

108. Puri N, Gardner JM, Brilliant MH. Aberrant pH of melanosomes in pink-eyed dilution (p) mutant melanocytes. J Invest Dermatol 2000; 115:607-13. [PMID: 10998131].

109. Manga P, Kromberg JGR, Box NF, Sturm RA, Jenkins T, Ramsay M. Rufous oculocutaneous albinism in southern African Blacks is caused by mutations in the TYRP1 gene. Am J Hum Genet 1997; 61:1095-101. [PMID: 9345097].

110. Sarangarajan R, Boissy RE. Tyrp1 and oculocutaneous albinism type 3. Pigment Cell Res 2001; 14:437-44. [PMID: 11775055].

111. Inagaki K, Suzuki T, Shimizu H, Ishii N, Umezawa Y, Tada J, Kikuchi N, Takata M, Takamori K, Kishibe M, Tanaka M, Miyamura Y, Ito S, Tomita Y. Oculocutaneous albinism type 4 is one of the most common types of albinism in Japan. Am J Hum Genet 2004; 74:466-71. [PMID: 14961451].

112. Newton JM, Cohen-Barak O, Hagiwara N, Gardner JM, Davisson MT, King RA, Brilliant MH. Mutations in the human orthologue of the mouse underwhite gene (uw) underlie a new form of oculocutaneous albinism, OCA4. Am J Hum Genet 2001; 69:981-8. [PMID: 11574907].

113. Liu Y, Chi W, Tao L, Wang G, Deepak RNVK, Sheng L, Chen T, Feng Y, Cao X, Cheng L, Zhao X, Liu X, Deng H, Fan H, Jiang P, Chen L. Ablation of proton/glucose exporter SLC45A2 enhances melanosomal glycolysis to inhibit melanin biosynthesis and promote melanoma metastasis. J Invest Dermatol 2022; 142:2744-2755.e9. [PMID: 35469906].

114. Kausar T, Bhatti MA, Ali M, Shaikh RS, Ahmed ZM. OCA5, a novel locus for non-syndromic oculocutaneous albinism, maps to chromosome 4q24. Clin Genet 2013; 84:91-3. [PMID: 23050561].

115. Wei A-H, Zang D-J, Zhang Z, Liu X-Z, He X, Yang L, Wang Y, Zhou Z-Y, Zhang M-R, Dai L-L, Yang X-M, Li W. Exome sequencing identifies SLC24A5 as a candidate gene for nonsyndromic oculocutaneous albinism. J Invest Dermatol 2013; 133:1834-40. [PMID: 23364476].

116. Lamason RL, Mohideen M-APK, Mest JR, Wong AC, Norton HL, Aros MC, Jurynec MJ, Mao X, Humphreville VR, Humbert JE, Sinha S, Moore JL, Jagadeeswaran P, Zhao W, Ning G, Makalowska I, McKeigue PM, O'donnell D, Kittles R, Parra EJ, Mangini NJ, Grunwald DJ, Shriver MD, Canfield VA, Cheng KC. SLC24A5, a putative cation exchanger, affects pigmentation in zebrafish and humans. Science 2005; 310:1782-6. [PMID: 16357253].

117. Ginger RS, Askew SE, Ogborne RM, Wilson S, Ferdinando D, Dadd T, Smith AM, Kazi S, Szerencsei RT, Winkfein RJ, Schnetkamp PPM, Green MR. SLC24A5 encodes a trans-Golgi network protein with potassium-dependent sodium-calcium exchange activity that regulates human epidermal melanogenesis. J Biol Chem 2008; 283:5486-95. [PMID: 18166528].

118. Grønskov K, Dooley CM, Østergaard E, Kelsh RN, Hansen L, Levesque MP, Vilhelmsen K, Møllgård K, Stemple DL, Rosenberg T. Mutations in c10orf11, a melanocyte-differentiation gene, cause autosomal-recessive albinism. Am J Hum Genet 2013; 92:415-21. [PMID: 23395477].

119. Beyers WC, Detry AM, Di Pietro SM. OCA7 is a melanosome membrane protein that defines pigmentation by regulating early stages of melanosome biogenesis. J Biol Chem 2022; 298:102669[PMID: 36334630].

120. Kruijt CC, de Wit GC, van Minderhout HM, Schalij-Delfos NE, van Genderen MM. Clinical and mutational characteristics of oculocutaneous albinism type 7. Sci Rep 2024; 14:7572-[PMID: 38555393].

121. Pennamen P, Tingaud-Sequeira A, Gazova I, Keighren M, McKie L, Marlin S, Gherbi Halem S, Kaplan J, Delevoye C, Lacombe D, Plaisant C, Michaud V, Lasseaux E, Javerzat S, Jackson I, Arveiler B. Dopachrome tautomerase variants in patients with oculocutaneous albinism. Genet Med 2021; 23:479-87. [PMID: 33100333].

122. Volk AE, Hedergott A, Preising M, Rading S, Fricke J, Herkenrath P, Nürnberg P, Altmüller J, von Ameln S, Lorenz B, Neugebauer A, Karsak M, Kubisch C. Biallelic mutations in L-dopachrome tautomerase (DCT) cause infantile nystagmus and oculocutaneous albinism. Hum Genet 2021; 140:1157-68. [PMID: 33959807].

123. Bouchard B, Del Marmol V, Jackson IJ, Cherif D, Dubertret L. Molecular characterization of a human tyrosinase-related-protein-2 cDNA. Patterns of expression in melanocytic cells. Eur J Biochem 1994; 219:127-34. [PMID: 8306979].

124. Leonard LJ, Townsend D, King RA. Function of dopachrome oxidoreductase and metal ions in dopachrome conversion in the eumelanin pathway. Biochemistry 1988; 27:6156-9. [PMID: 3142518].

125. Kroumpouzos G, Urabe K, Kobayashi T, Sakai C, Hearing VJ. Functional analysis of the slaty gene product (TRP2) as dopachrome tautomerase and the effect of a point mutation on its catalytic function. Biochem Biophys Res Commun 1994; 202:1060-8. [PMID: 8048919].

126. Hermansky F, Pudlak P. Albinism associated with hemorrhagic diathesis and unusual pigmented reticular cells in the bone marrow: report of two cases with histochemical studies. Blood 1959; 14:162-9. [PMID: 13618373].

127. Gochuico BR, Huizing M, Golas GA, Scher CD, Tsokos M, Denver SD, Frei-Jones MJ, Gahl WA. Interstitial lung disease and pulmonary fibrosis in Hermansky-Pudlak syndrome type 2, an adaptor protein-3 complex disease. Mol Med 2012; 18:56-64. [PMID: 22009278].

128. Schinella RA, Greco MA, Cobert BL, Denmark LW, Cox RP. Hermansky-Pudlak syndrome with granulomatous colitis. Ann Intern Med 1980; 92:20-3. [PMID: 7350869].

129. Fontana S, Parolini S, Vermi W, Booth S, Gallo F, Donini M, Benassi M, Gentili F, Ferrari D, Notarangelo LD, Cavadini P, Marcenaro E, Dusi S, Cassatella M, Facchetti F, Griffiths GM, Moretta A, Notarangelo LD, Badolato R. Innate immunity defects in Hermansky-Pudlak type 2 syndrome. Blood 2006; 107:4857-64. [PMID: 16507770].

130. Huizing M, Helip-Wooley A, Westbroek W, Gunay-Aygun M, Gahl WA. Disorders of lysosome-related organelle biogenesis: clinical and molecular genetics. Annu Rev Genomics Hum Genet 2008; 9:359-86. [PMID: 18544035].

131. Bowman SL, Bi-Karchin J, Le L, Marks MS. The road to lysosome-related organelles: Insights from Hermansky-Pudlak syndrome and other rare diseases. Traffic 2019; 20:404-35. [PMID: 30945407].

132. Pennamen P, Le L, Tingaud-Sequeira A, Fiore M, Bauters A, Van Duong Béatrice N, Coste V, Bordet J-C, Plaisant C, Diallo M, Michaud V, Trimouille A, Lacombe D, Lasseaux E, Delevoye C, Picard FM, Delobel B, Marks MS, Arveiler B. BLOC1S5 pathogenic variants cause a new type of Hermansky-Pudlak syndrome. Genet Med 2020; 22:1613-22. [PMID: 32565547].

133. Di Pietro SM, Falcón-Pérez JM, Dell'Angelica EC. Characterization of BLOC-2, a complex containing the Hermansky-Pudlak syndrome proteins HPS3, HPS5 and HPS6. Traffic 2004; 5:276-83. [PMID: 15030569].

134. Oh J, Ho L, Ala-Mello S, Amato D, Armstrong L, Bellucci S, Carakushansky G, Ellis JP, Fong CT, Green JS, Heon E, Legius E, Levin AV, Nieuwenhuis HK, Pinckers A, Tamura N, Whiteford ML, Yamasaki H, Spritz RA. Mutation analysis of patients with Hermansky-Pudlak syndrome: a frameshift hot spot in the HPS gene and apparent locus heterogeneity. Am J Hum Genet 1998; 62:593-8. [PMID: 9497254].

135. Suzuki T, Li W, Zhang Q, Karim A, Novak EK, Sviderskaya EV, Hill SP, Bennett DC, Levin AV, Nieuwenhuis HK, Fong CT, Castellan C, Miterski B, Swank RT, Spritz RA. Hermansky-Pudlak syndrome is caused by mutations in HPS4, the human homolog of the mouse light-ear gene. Nat Genet 2002; 30:321-4. [PMID: 11836498].

136. Benvenuto L, Qayum S, Kim H, Robbins H, Shah L, Dimango A, Magda G, Grewal H, Lemaitre P, Stanifer BP, Sonett J, D'Ovidio F, Arcasoy SM. Lung transplantation for pulmonary fibrosis associated with Hermansky-Pudlak syndrome. A single-center experience. Transplant Direct 2022; 8:e1303[PMID: 35350109].

137. de Boer M, van Leeuwen K, Geissler J, van Alphen F, de Vries E, van der Kuip M, Terheggen SWJ, Janssen H, van den Berg TK, Meijer AB, Roos D, Kuijpers TW. Hermansky-Pudlak syndrome type 2: Aberrant pre-mRNA splicing and mislocalization of granule proteins in neutrophils. Hum Mutat 2017; 38:1402-11. [PMID: 28585318].

138. Ammann S, Schulz A, Krägeloh-Mann I, Dieckmann NM, Niethammer K, Fuchs S, Eckl KM, Plank R, Werner R, Altmüller J, Thiele H, Nürnberg P, Bank J, Strauss A, von Bernuth H, Zur Stadt U, Grieve S, Griffiths GM, Lehmberg K, Hennies HC, Ehl S. Mutations in AP3D1 associated with immunodeficiency and seizures define a new type of Hermansky-Pudlak syndrome. Blood 2016; 127:997-1006. [PMID: 26744459].

139. Spritz RA. Multi-organellar disorders of pigmentation: tied up in traffic. Clin Genet 1999; 55:309-17. [PMID: 10422800].

140. Nagle DL, Karim MA, Woolf EA, Holmgren L, Bork P, Misumi DJ, McGrail SH, Dussault BJ Jr, Perou CM, Boissy RE, Duyk GM, Spritz RA, Moore KJ. Identification and mutation analysis of the complete gene for Chediak-Higashi syndrome. Nat Genet 1996; 14:307-11. [PMID: 8896560].

141. Karim MA, Suzuki K, Fukai K, Oh J, Nagle DL, Moore KJ, Barbosa E, Falik-Borenstein T, Filipovich A, Ishida Y, Kivrikko S, Klein C, Kreuz F, Levin A, Miyajima H, Regueiro JR, Russo C, Uyama E, Vierimaa O, Spritz RA. Apparent genotype-phenotype correlation in childhood, adolescent, and adult Chediak-Higashi syndrome. Am J Med Genet 2002; 108:16-22. [PMID: 11857544].

142. Greene S, Soldatos A, Toro C, Zein WM, Snow J, Lehky TJ, Malicdan MCV, Introne WJ. Chedíak-Higashi Syndrome: Hair-to-toe spectrum. Semin Pediatr Neurol 2024; 52:101168[PMID: 39622608].

143. Kohl S, Zobor D, Chiang WC, Weisschuh N, Staller J, Gonzalez Menendez I, Chang S, Beck SC, Garcia Garrido M, Sothilingam V, Seeliger MW, Stanzial F, Benedicenti F, Inzana F, Héon E, Vincent A, Beis J, Strom TM, Rudolph G, Roosing S, Hollander AI, Cremers FPM, Lopez I, Ren H, Moore AT, Webster AR, Michaelides M, Koenekoop RK, Zrenner E, Kaufman RJ, Tsang SH, Wissinger B, Lin JH. Mutations in the unfolded protein response regulator ATF6 cause the cone dysfunction disorder achromatopsia. Nat Genet 2015; 47:757-65. [PMID: 26029869].

144. Ren X, Huang L, Cheng S, Wang J, Li N. Novel pathogenic variants of SLC38A8 gene and literature review. Eur J Ophthalmol 2024; 34:1740-9. [PMID: 38515398].

145. Kim S, Lowe A, Dharmat R, Lee S, Owen LA, Wang J, Shakoor A, Li Y, Morgan DJ, Hejazi AA, Cvekl A, DeAngelis MM, Zhou ZJ, Chen R, Liu W. Generation, transcriptome profiling, and functional validation of cone-rich human retinal organoids. Proc Natl Acad Sci U S A 2019; 116:10824-33. [PMID: 31072937].

146. Bakker R, Wagstaff EL, Kruijt CC, Emri E, van Karnebeek CDM, Hoffmann MB, Brooks BP, Boon CJF, Montoliu L, van Genderen MM, Bergen AA. The retinal pigmentation pathway in human albinism: Not so black and white. Prog Retin Eye Res 2022; 91:101091[PMID: 35729001].

147. Smirnov VM, Lasseaux E, Michaud V, Courdier C, Meunier I, Arveiler B, Defoort-Dhellemmes S. Crossed VEP asymmetry in a patient with AHR-linked infantile nystagmus and foveal hypoplasia. Doc Ophthalmol 2024; 149:47-52. [PMID: 38922562].

148. Chevallier A, Mialot A, Petit JM, Fernandez-Salguero P, Barouki R, Coumoul X, Beraneck M. Oculomotor deficits in aryl hydrocarbon receptor null mouse. PLoS One 2013; 8:e53520[PMID: 23301081].

149. Thomas MG, Crosier M, Lindsay S, Kumar A, Araki M, Leroy BP, McLean RJ, Sheth V, Maconachie G, Thomas S, Moore AT, Gottlob I. Abnormal retinal development associated with FRMD7 mutations. Hum Mol Genet 2014; 23:4086-93. [PMID: 24688117].

150. Jordan T, Hanson I, Zaletayev D, Hodgson S, Prosser J, Seawright A, Hastie N, van Heyningen V. The human PAX6 gene is mutated in two patients with aniridia. Nat Genet 1992; 1:328-32. [PMID: 1302030].

151. Kleinjan DA, Seawright A, Schedl A, Quinlan RA, Danes S, van Heyningen V. Aniridia-associated translocations, DNase hypersensitivity, sequence comparison and transgenic analysis redefine the functional domain of PAX6. Hum Mol Genet 2001; 10:2049-59. [PMID: 11590122].

152. Jalkanen R, Bech-Hansen NT, Tobias R, Sankila EM, Mäntyjärvi M, Forsius H, de la Chapelle A, Alitalo T. A novel CACNA1F gene mutation causes Aland Island eye disease. Invest Ophthalmol Vis Sci 2007; 48:2498-502. [PMID: 17525176].

153. Smahi A, Courtois G, Vabres P, Yamaoka S, Heuertz S, Munnich A, Israël A, Heiss NS, Klauck SM, Kioschis P, Wiemann S, Poustka A, Esposito T, Bardaro T, Gianfrancesco F, Ciccodicola A, D'Urso M, Woffendin H, Jakins T, Donnai D, Stewart H, Kenwrick SJ, Aradhya S, Yamagata T, Levy M, Lewis RA, Nelson DL. The International Incontinentia Pigmenti (IP) Consortium. Genomic rearrangement in NEMO impairs NF-kappaB activation and is a cause of incontinentia pigmenti. Nature 2000; 405:466-72. [PMID: 10839543].

154. Basilius J, Young MP, Michaelis TC, Hobbs R, Jenkins G, Hartnett ME. Structural abnormalities of the inner macula in incontinentia pigmenti. JAMA Ophthalmol 2015; 133:1067-72. [PMID: 26043102].

155. Ju Y, Zhang L, Gao F, Zong Y, Chen T, Ruan L, Chang Q, Zhang T, Huang X. Genetic characteristics and clinical manifestations of foveal hypoplasia in familial exudative vitreoretinopathy. Am J Ophthalmol 2024; 262:73-85. [PMID: 38280677].

156. Alshamrani AA, Magliyah M, Alkuraya FS, Alabdi L, Alfaadhel TA, Alsulaiman SM. Early-onset myopia and retinal detachment without typical microcoria or severe proteinuria due to a novel LAMB2 variant. Ophthalmol Retina 2024; 8:155-62. [PMID: 37678612].

157. Siu VM, Ratko S, Prasad AN, Prasad C, Rupar CA. Amish microcephaly: Long-term survival and biochemical characterization. Am J Med Genet A 2010; 152A:1747-51. [PMID: 20583149].

158. Ye M, Berry-Wynne KM, Asai-Coakwell M, Sundaresan P, Footz T, French CR, Abitbol M, Fleisch VC, Corbett N, Allison WT, Drummond G, Walter MA, Underhill TM, Waskiewicz AJ, Lehmann OJ. Mutation of the bone morphogenetic protein GDF3 causes ocular and skeletal anomalies. Hum Mol Genet 2010; 19:287-98. [PMID: 19864492].

159. Raviv S, Bharti K, Rencus-Lazar S, Cohen-Tayar Y, Schyr R, Evantal N, Meshorer E, Zilberberg A, Idelson M, Reubinoff B, Grebe R, Rosin-Arbesfeld R, Lauderdale J, Lutty G, Arnheiter H, Ashery-Padan R. PAX6 regulates melanogenesis in the retinal pigmented epithelium through feed-forward regulatory interactions with MITF. PLoS Genet 2014; 10:e1004360[PMID: 24875170].

160. Lopez VM, Decatur CL, Stamer WD, Lynch RM, McKay BS. L-DOPA is an endogenous ligand for OA1. PLoS Biol 2008; 6:e236[PMID: 18828673].

161. Barnstable CJ, Tombran-Tink J. Neuroprotective and antiangiogenic actions of PEDF in the eye: molecular targets and

therapeutic potential. Prog Retin Eye Res 2004; 23:561-77. [PMID: 15302351].

162. Jablonski MM, Tombran-Tink J, Mrazek DA, Iannaccone A. Pigment epithelium-derived factor supports normal development of photoreceptor neurons and opsin expression after retinal pigment epithelium removal. J Neurosci 2000; 20:7149-57. [PMID: 11007870].

163. Tombran-Tink J, Shivaram SM, Chader GJ, Johnson LV, Bok D. Expression, secretion, and age-related downregulation of pigment epithelium-derived factor, a serpin with neurotrophic activity. J Neurosci 1995; 15:4992-5003. [PMID: 7623128].

164. Subramanian P, Locatelli-Hoops S, Kenealey J, DesJardin J, Notari L, Becerra SP. Pigment epithelium-derived factor (PEDF) prevents retinal cell death via PEDF Receptor (PEDF-R): identification of a functional ligand binding site. J Biol Chem 2013; 288:23928-42. [PMID: 23818523].

165. Cortese K, Giordano F, Surace EM, Venturi C, Ballabio A, Tacchetti C, Marigo V. The ocular albinism type 1 (OA1) gene controls melanosome maturation and size. Invest Ophthalmol Vis Sci 2005; 46:4358-64. [PMID: 16303920].

166. Falletta P, Bagnato P, Bono M, Monticone M, Schiaffino MV, Bennett DC, Goding CR, Tacchetti C, Valetti C. Melanosome-autonomous regulation of size and number: the OA1 receptor sustains PMEL expression. Pigment Cell Melanoma Res 2014; 27:565-79. [PMID: 24650003].

167. Rapaport DH, Stone J. The area centralis of the retina in the cat and other mammals: focal point for function and development of the visual system. Neuroscience 1984; 11:289-301. [PMID: 6425714].

168. da Silva S, Cepko CL. Fgf8 expression and degradation of retinoic acid are required for patterning a high-acuity area of the retina. Dev Cell 2017; 42:68-81.e6. [PMID: 28648799].

169. O'Day K. The fundus and fovea centralis of the albatross (Diomedea cauta cauta-gould). Br J Ophthalmol 1940; 24:201-7. [PMID: 18169690].

170. Mitkus M, Olsson P, Toomey MB, Corbo JC, Kelber A. Specialized photoreceptor composition in the raptor fovea. J Comp Neurol 2017; 525:2152-63. [PMID: 28199005].

171. Querubin A, Lee HR, Provis JM, O'Brien KM. Photoreceptor and ganglion cell topographies correlate with information convergence and high acuity regions in the adult pigeon (Columba livia) retina. J Comp Neurol 2009; 517:711-22. [PMID: 19827162].

172. Collin SP, Collin HB. The foveal photoreceptor mosaic in the pipefish, Corythoichthyes paxtoni (Syngnathidae, Teleostei). Histol Histopathol 1999; 14:369-82. [PMID: 10212798].

173. Röll B. Retina of Bouton's skink (Reptilia, Scincidae): visual cells, fovea, and ecological constraints. J Comp Neurol 2001; 436:487-96. [PMID: 11447591].

174. Makaretz M, Levine RL. A light microscopic study of the bifoveate retina in the lizard Anolis carolinensis: general observations and convergence ratios. Vision Res 1980; 20:679-86. [PMID: 7445438].

175. Lovern MB, Holmes MM, Wade J. The green anole (Anolis carolinensis): a reptilian model for laboratory studies of reproductive morphology and behavior. ILAR J 2004; 45:54-64. [PMID: 14756155].

176. Wahle MA, Kim HQ, Menke DB, Lauderdale JD, Rasys AM. Maturation and refinement of the maculae and foveae in the Anolis sagrei lizard. Exp Eye Res 2023; 234:109611[PMID: 37536437].

177. Alföldi J, Di Palma F, Grabherr M, Williams C, Kong L, Mauceli E, Russell P, Lowe CB, Glor RE, Jaffe JD, Ray DA, Boissinot S, Shedlock AM, Botka C, Castoe TA, Colbourne JK, Fujita MK, Moreno RG, ten Hallers BF, Haussler D, Heger A, Heiman D, Janes DE, Johnson J, de Jong PJ, Koriabine MY, Lara M, Novick PA, Organ CL, Peach SE, Poe S, Pollock DD, de Queiroz K, Sanger T, Searle S, Smith JD, Smith Z, Swofford R, Turner-Maier J, Wade J, Young S, Zadissa A, Edwards SV, Glenn TC, Schneider CJ, Losos JB, Lander ES, Breen M, Ponting CP, Lindblad-Toh K. The genome of the green anole lizard and a comparative analysis with birds and mammals. Nature 2011; 477:587-91. [PMID: 21881562].

178. Tollis M, Hutchins ED, Stapley J, Rupp SM, Eckalbar WL, Maayan I, Lasku E, Infante CR, Dennis SR, Robertson JA, May CM, Crusoe MR, Bermingham E, DeNardo DF, Hsieh ST, Kulathinal RJ, McMillan WO, Menke DB, Pratt SC, Rawls JA, Sanjur O, Wilson-Rawls J, Wilson Sayres MA, Fisher RE, Kusumi K. Comparative Genomics Reveals Accelerated Evolution in Conserved Pathways during the Diversification of Anole Lizards. Genome Biol Evol 2018; 10:489-506. [PMID: 29360978].

179. Sanger TJ, Losos JB, Gibson-Brown JJ. A developmental staging series for the lizard genus Anolis: a new system for the integration of evolution, development, and ecology. J Morphol 2008; 269:129-37. [PMID: 17724661].

180. Sannan NS, Shan X, Gregory-Evans K, Kusumi K, Gregory-Evans CY. Anolis carolinensis as a model to understand the molecular and cellular basis of foveal development. Exp Eye Res 2018; 173:138-47. [PMID: 29775563].

181. Fite KV, Lister BC. Bifoveal vision in anolis lizards. Brain Behav Evol 1981; 19:144-54. [PMID: 7326573].

182. Locket NA. Problems of deep foveas. Aust N Z J Ophthalmol 1992; 20:281-95. [PMID: 1295523].

183. Fleishman LJ. Lizard visual ecology. Front Amphib Reptile Sci 2024; 2:1426675.

184. Trieschmann M, van Kuijk FJGM, Alexander R, Hermans P, Luthert P, Bird AC, Pauleikhoff D. Macular pigment in the human retina: histological evaluation of localization and distribution. Eye (Lond) 2008; 22:132-7. [PMID: 17401321].

185. Rasys AM, Pau SH, Irwin KE, Luo S, Kim HQ, Wahle MA, Menke DB, Lauderdale JD. Histological analysis of retinal development and remodeling in the brown anole lizard (Anolis sagrei). J Anat 2025; 246:1019-33. [PMID: 39726164].

186. Douglas RM, Alam NM, Silver BD, McGill TJ, Tschetter WW, Prusky GT. Independent visual threshold measurements in

the two eyes of freely moving rats and mice using a virtual-reality optokinetic system. Vis Neurosci 2005; 22:677-84. [PMID: 16332278].

187. Gregory-Evans CY, Wang X, Wasan KM, Zhao J, Metcalfe AL, Gregory-Evans K. Postnatal manipulation of Pax6 dosage reverses congenital tissue malformation defects. J Clin Invest 2014; 124:111-6. [PMID: 24355924].

188. Mitani N, Anyoji K, Uzuki Y, Taga K. Feasibility of bait attraction in the green anole (Anolis carolinensis). Curr Herpetol 2015; 34:164-71. .

189. Rasys AM, Park S, Ball RE, Alcala AJ, Lauderdale JD, Menke DB. CRISPR-Cas9 gene editing in lizards through microinjection of unfertilized oocytes. Cell Rep 2019; 28:2288-2292.e3. [PMID: 31461646].

190. Abe T, Kaneko M, Kiyonari H. A reverse genetic approach in geckos with the CRISPR/Cas9 system by oocyte microinjection. Dev Biol 2023; 497:26-32. [PMID: 36868446].

191. Sabin CE, Rasys A, Osman R, Trainor P, Menke DB, Lauderdale JD. Investigating the role of ocular shape changes in fovea development in chameleons along with wild-type and albino lizards. Invest Ophthalmol Vis Sci 2012; 62:1696-.

192. Grainger RM, Lauderdale JD, Collins JL, Trout KL, McCullen Krantz S, Wolfe SS, Netland PA. Report on the 2021 Aniridia North America symposium on PAX6, aniridia, and beyond. Ocul Surf 2023; 29:423-31. [PMID: 37247841].

193. Kroeger H, Sabin C, Holub JA, Menke DB, Lauderdale JD. Absence of cone photoreceptor outer segments in atf6-/- anole lizards – a new research model for cone dystrophies. Invest Ophthalmol Vis Sci 2023; 64:3214-.

194. Jeffery G. The albino retina: an abnormality that provides insight into normal retinal development. Trends Neurosci 1997; 20:165-9. [PMID: 9106357].

195. Lavado A, Jeffery G, Tovar V, de la Villa P, Montoliu L. Ectopic expression of tyrosine hydroxylase in the pigmented epithelium rescues the retinal abnormalities and visual function common in albinos in the absence of melanin. J Neurochem 2006; 96:1201-11. [PMID: 16445854].

196. Summers CG, Connett JE, Holleschau AM, Anderson JL, De Becker I, McKay BS, Brilliant MH. Does levodopa improve vision in albinism? Results of a randomized, controlled clinical trial. Clin Exp Ophthalmol 2014; 42:713-21. [PMID: 24641678].

197. Lee H, Purohit R, Sheth V, Maconachie G, Tu Z, Thomas MG, Pilat A, McLean RJ, Proudlock FA, Gottlob I. Retinal development in infants and young children with albinism: Evidence for plasticity in early childhood. Am J Ophthalmol 2023; 245:202-11. [PMID: 36084688].

198. Lee H, Scott J, Griffiths H, Self JE, Lotery A. Oral levodopa rescues retinal morphology and visual function in a murine model of human albinism. Pigment Cell Melanoma Res 2019; 32:657-71. [PMID: 30851223].

199. Sanchez-Bretano A, Keeling E, Scott JA, Lynn SA, Soundara-Pandi SP, Macdonald SL, Newall T, Griffiths H, Lotery AJ, Ratnayaka JA, Self JE, Lee H. Human equivalent doses of L-DOPA rescues retinal morphology and visual function in a murine model of albinism. Sci Rep 2023; 13:17173-[PMID: 37821525].

200. Ferenchak K, Deitch I, Huckfeldt R. Antisense oligonucleotide therapy for ophthalmic conditions. Semin Ophthalmol 2021; 36:452-7. [PMID: 34010086].

201. Cloutier F, Lawrence M, Goody R, Lamoureux S, Al-Mahmood S, Colin S, Ferry A, Conduzorgues JP, Hadri A, Cursiefen C, Udaondo P, Viaud E, Thorin E, Chemtob S. Antiangiogenic activity of aganirsen in nonhuman primate and rodent models of retinal neovascular disease after topical administration. Invest Ophthalmol Vis Sci 2012; 53:1195-203. [PMID: 22323484].

202. Hyman MJ, Skondra D, Aggarwal N, Moir J, Boucher N, McKay BS, MacCumber MW, Lavine JA. Levodopa is associated with reduced development of neovascular age-related macular degeneration. Ophthalmol Retina 2023; 7:745-52. [PMID: 37146684].

203. Chan KS, Aggarwal N, Lawson S, Boucher N, MacCumber MW, Lavine JA. Levodopa is associated with reduced development of new-onset geographic atrophy in patients with age-related macular degeneration. Eye Vis (Lond) 2024; 11:44-[PMID: 39501348].

204. Rao S, Xiao K, Chen X, Sun X. Dopamine alleviated diabetic retinal neurodegeneration through protecting retinal ganglion cells from ferroptosis via the Nrf2/HO-1 signaling pathway. ACS Omega 2025; 10:30397-410. [PMID: 40727724].

Articles are provided courtesy of Emory University and The Abraham J. & Phyllis Katz Foundation. The print version of this article was created on 3 October 2025. This reflects all typographical corrections and errata to the article through that date. Details of any changes may be found in the online version of the article.